HHS Public Access

Author manuscript

Mol Microbiol. Author manuscript; available in PMC 2021 October 01.

Published in final edited form as:

Mol Microbiol. 2020 October ; 114(4): 563–581. doi:10.1111/mmi.14560.

Channels modestly impact compartment-specific ATP levels during *Bacillus subtilis* sporulation and a rise in the mother cell ATP level is not necessary for Pro-σ^K cleavage

Daniel Parrell, **Lee Kroos***

Department of Biochemistry and Molecular Biology, Michigan State University, East Lansing, Michigan, USA

Summary

Starvation of *Bacillus subtilis* initiates endosporulation involving formation of mother cell (MC) and forespore (FS) compartments. During engulfment, the MC membrane migrates around the FS and protein channels connect the two compartments. The channels are necessary for post-engulfment FS gene expression, which relieves inhibition of SpoIVFB, an intramembrane protease that cleaves Pro-σ^K, releasing σ^K into the MC. SpoIVFB has an ATP-binding domain exposed to the MC cytoplasm, but the role of ATP in regulating Pro-σ^K cleavage has been unclear, as has the impact of the channels on MC and FS ATP levels. Using luciferase produced separately in each compartment to measure relative ATP concentrations during sporulation, we found that the MC ATP concentration rises about twofold coincident with increasing cleavage of Pro-σ^K, and the FS ATP concentration does not decline. Mutants lacking a channel protein or defective in channel protein turnover exhibited modest and varied effects on ATP levels, which suggested that low ATP concentration does not explain the lack of post-engulfment FS gene expression in channel mutants. Furthermore, a rise in the MC ATP level was not necessary for Pro-σ^K cleavage by SpoIVFB, based on analysis of mutants that bypass the need for relief of SpoIVFB inhibition.

Graphical Abstract

*For correspondence. kroos@msu.edu; Tel. (+1) 517 355 9726; Fax (+1) 517 353 9334.

Author contributions

Conception or design of the study: DP, LK

Acquisition, analysis, and interpretation of the data: DP, LK

Writing of the manuscript: DP, LK

Data availability statement

The data that support the findings of this study are available from the corresponding author upon reasonable request.

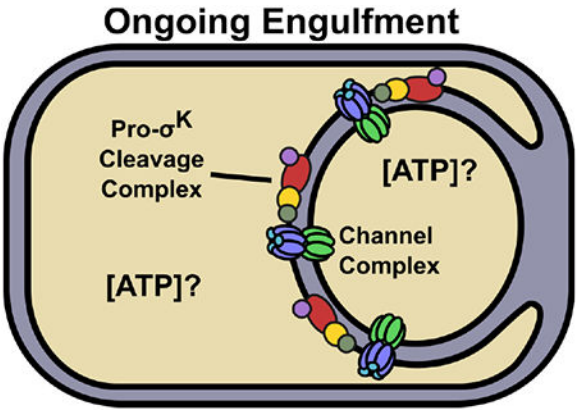

Abbreviated summary

During *Bacillus subtilis* endosporulation, the mother cell membrane engulfs the forespore and channel complexes form that may impact ATP concentrations in the compartments. Upon engulfment completion, channel destruction occurs and the Pro-σ^K cleavage complex is activated. The mother cell ATP concentration was found to increase twofold coincident with channel protein loss, but this was not required to activate Pro-σ^K cleavage.

Keywords

adenosine triphosphate; Bacillus subtilis; spores; sigma factor; signal transduction; gene expression regulation

Introduction

Endospore formation by the bacterium *Bacillus subtilis* has long been a model system for studies of cell-to-cell communication in bacteria (Losick & Stragier, 1992). The rod-shaped cells initiate a remarkably complex sporulation process upon encountering starvation conditions (Tan & Ramamurthi, 2014). A polar septum is formed, creating a large compartment referred to as the mother cell (MC) and a smaller compartment destined to become the forespore (FS). Next, the MC membrane migrates around the FS during the process of engulfment, eventually pinching off the FS within the MC (Fig. 1). At this stage, the FS compartment is surrounded by two membranes, separated by an intermembrane space. Following engulfment, a modified peptidoglycan layer called the cortex is produced in the intermembrane space and a protective protein coat is produced by the MC around the FS. Once FS development is complete, the MC lyses, releasing a dormant spore.

B. subtilis sporulation is controlled by differential gene expression in the two compartments, driven by the activation of alternative sigma factors (Higgins & Dworkin, 2012, Kroos, 2007). Several mechanisms ensure activation of σ^F in the FS shortly after polar septum formation (Bradshaw & Losick, 2015). Activity of σ^F initiates a signaling pathway that leads to proteolytic activation of Pro-σ^E in the MC (Konovalova et al., 2014). During the ensuing engulfment process, σ^F activity produces SpoIIQ, which inserts in the inner FS membrane, and σ^E activity produces SpoIIIA proteins, which insert in the engulfing MC membrane

(Fig. 1, left side), forming channels between the two compartments that are required for full activity of σ^G in the FS and maintenance of FS integrity (Blaylock et al., 2004, Doan et al., 2005, Camp & Losick, 2008, Meisner et al., 2008, Camp & Losick, 2009, Doan et al., 2009, Mearls et al., 2018). The activation of σ^G coincides with completion of engulfment and initiates a signaling pathway that leads to proteolytic cleavage of Pro-σ^K to active σ^K in the MC (Kroos & Akiyama, 2013, Konovalova et al., 2014).

Intercellular communication is an essential function for multicellularity. In animals and plants, gap junctions and plasmodesmata, respectively, provide channels for passage of small molecules between cells. The channels that form between the MC and the FS during the engulfment stage of *B. subtilis* sporulation have been proposed to function analogously (Camp & Losick, 2009, Doan et al., 2009). Specifically, the MC has been proposed to provide metabolites and/or osmolytes through the channels during engulfment that support post-engulfment FS biosynthesis and integrity. Evidence for this “feeding tube model” is that the channels are required not only for full activity of σ^G in the FS, but for persistent activity of σ^F in the absence of σ^G and for activity of heterologous phage T7 RNA polymerase produced in the FS, as measured by expression of *lacZ* fusion reporters (Camp & Losick, 2009). These findings support a general requirement of the channels for post-engulfment FS transcription and/or translation. Channel function is also necessary to prevent FS collapse after completion of engulfment, and this does not require σ^G (Doan et al., 2009). However, the identity of the small molecule(s) proposed to transit the channels is unknown. Similarity of SpoIIIA proteins to components of protein secretion systems suggested that the channels might transport a protein from the MC to the FS (Camp & Losick, 2008, Meisner et al., 2008). A third possibility is that the channels play a structural role in maintaining FS morphology, which is required for post-engulfment FS gene expression (Rodrigues et al., 2016a). In *Clostridium difficile*, proteins similar to SpoIIQ and the SpoIIIA proteins of *B. subtilis* are important for normal FS morphology, but are dispensable for at least a portion of σ^G-dependent FS gene expression (Fimlaid et al., 2015, Serrano et al., 2016).

The extracytoplasmic domains of SpoIIQ and SpoIIIAH interact directly, forming a channel in the intermembrane space surrounding the FS (Blaylock et al., 2004, Doan et al., 2005). The channel appears to be gated on the MC (SpoIIIAH) side by other SpoIIIA proteins and open on the FS (SpoIIQ) side (Meisner et al., 2008). SpoIIIAA may function in substrate transport, since it resembles secretion ATPases (Meisner et al., 2008) and its ATPase motifs appear to be required for σ^G activation (Doan et al., 2009). The eight SpoIIIA proteins and SpoIIQ form a multimeric complex, which also includes GerM (Camp & Losick, 2008, Meisner et al., 2008, Zeytuni et al., 2018, Rodrigues et al., 2016b). Structural determination and modeling of channel protein complexes support the notion that they form large, stacked rings capable of mediating communication and/or a structural connection between the MC and FS (Rodrigues et al., 2016a, Zeytuni et al., 2017, Levdikov et al., 2012, Trouve et al., 2018, Meisner et al., 2012).

Upon completion of engulfment, the channels likely cease to function. SpoIIQ is released from immobile complexes and cleaved by SpoIVB (Chiba et al., 2007). SpoIIIAH is rapidly degraded (Meisner et al., 2008). The levels of SpoIIIAA and SpoIIIAE decline (Doan et al., 2009).

Although the function of the channels remains a mystery, we reasoned that channel function may impact compartment-specific ATP levels. One possibility is illustrated in Figure 1. During engulfment, channel function may maintain a similar ATP concentration in the two compartments (top left). Upon completion of engulfment, loss of channel function may increase the ATP level in the MC and decrease the ATP level in the FS (top right), since FS ATP would continue to be utilized for gene expression, translation, and maintenance of integrity. While it is possible that ATP itself is transported by the channels, this need not be the case for channel function to affect compartment-specific ATP levels. To investigate whether channel function affects MC and FS ATP levels, we devised a method to measure the relative ATP concentration in each compartment during sporulation. The method relies on compartment-specific synthesis of firefly luciferase (Luc), which catalyzes the ATP-dependent oxidation of luciferin, producing light (Branchini et al., 1999). Luc has been used to measure the relative ATP concentration in *Escherichia coli* (Schneider & Gourse, 2004), and as a reporter of promoter activity during *B. subtilis* growth and sporulation (Mirouze et al., 2011), but Luc has not been used to measure relative ATP levels in the two compartments.

If the loss of channel function upon engulfment completion causes the MC ATP concentration to rise, it may act as a signal to stimulate proteolytic cleavage of Pro-σ^K to active σ^K by SpoIVFB in the MC (Kroos & Akiyama, 2013, Konovalova et al., 2014) (Fig. 1, right side). SpoIVFB is an intramembrane metalloprotease (Rudner et al., 1999, Yu & Kroos, 2000) with a cystathionine-β-synthase (CBS) domain that binds ATP *in vitro*, and cleavage of Pro-σ^K by SpoIVFB *in vitro* depends on ATP (Zhou et al., 2009). The CBS domain of SpoIVFB is predicted to be exposed to the MC cytoplasm (Fig. 1, bottom), based on membrane topological analysis in *E. coli* (Green & Cutting, 2000). CBS domains in a variety of proteins regulate activity in response to energy status by undergoing a conformational change upon ligand binding (Baykov et al., 2011, Scott et al., 2004). Hence, it was proposed that the CBS domain of SpoIVFB senses the ATP concentration in the MC and regulates Pro-σ^K cleavage appropriately (Zhou et al., 2009). Deletion of the SpoIVFB CBS domain resulted in no cleavage of Pro-σ^K upon co-production in *E. coli* (Halder et al., 2017, Zhou et al., 2009). Co-production in *E. coli* of full-length, catalytically-inactive SpoIVFB with C-terminally truncated Pro-σ^K resulted in formation of a stable complex (Zhang et al., 2016). Cross-linking of the purified complex (Halder et al., 2017, Zhang et al., 2016) and of the two proteins co-synthesized in *E. coli* (Zhang et al., 2013) provided constraints to build a homology model of the complex, which suggested that ATP-induced movement of the SpoIVFB CBS domain might position Pro-σ^K for cleavage (Halder et al., 2017). However, in a recent study, a SpoIVFB-YFP fusion protein lacking the CBS domain cleaved Pro-σ^K during sporulation of *B. subtilis* (Ramirez-Guadiana et al., 2018). Cleavage was reduced, indicating that YFP can substitute for the CBS domain, albeit imperfectly. It remains to be established whether the SpoIVFB CBS domain senses the MC ATP concentration and regulates Pro-σ^K cleavage.

In addition to potential regulation of SpoIVFB by ATP binding to its CBS domain in the MC, SpoIVFB is regulated by a signaling pathway initiated by σ^G in the FS. This pathway involves two serine proteases, SpoIVB and CtpB, produced under σ^G control and secreted into the intermembrane space (Cutting et al., 1991a, Wakeley et al., 2000, Zhou & Kroos,

2005, Campo & Rudner, 2006, Campo & Rudner, 2007). SpoIVB and CtpB cleave SpoIVFA and BofA, which form an inhibitory complex with SpoIVFB (Cutting et al., 1990, Cutting et al., 1991b, Ricca et al., 1992, Rudner & Losick, 2002, Zhou & Kroos, 2004) (Fig. 1, bottom left). Recent evidence suggests that relief from inhibition induces a conformational change in SpoIVFB that promotes interaction with Pro-σ^K and cleavage to produce σ^K (Ramirez-Guadiana et al., 2018). Interestingly, the Pro-σ^K cleavage complexes co-localize with the channel complexes composed of SpoIIIA proteins and SpoIIQ (Doan et al., 2005, Jiang et al., 2005) (Fig. 1, left side). Interactions between proteins in the two complexes aid in recruitment to the membranes surrounding the FS, but neither the molecular details of the interactions nor whether they play a role beyond recruitment is known.

Here, we report the use of compartment-specific production of Luc to measure relative ATP levels in the MC and the FS of wild-type (WT) cells and mutants, including in the presence of inhibitors, to address several outstanding questions. Do ATP concentrations in the MC and FS change during sporulation? Do channel proteins impact the MC and FS ATP concentrations? If the MC ATP concentration does increase upon completion of engulfment and loss of channel function (Fig. 1, top right), is the elevated ATP level necessary for SpoIVFB to cleave Pro-σ^K?

Results

A Luc variant can detect changes in the ATP concentration in the mother cell and the forespore

DNA constructs were built in which the gene for Luc or an H245F variant (Luc H245F, which increases the K_m for Mg-ATP from 160 μM to 830 μM) (Branchini et al., 1999) were fused to the mother cell-specific *spoIID* promoter or to the forespore-specific *spoIIQ* promoter (Sharp & Pogliano, 2002) in plasmids that allow gene replacement by homologous recombination at the chromosomal *amyE* locus of *B. subtilis* (Shimotsu & Henner, 1986). The resulting strains were used to test the sensitivity of Luc and Luc H245F to decreases in the ATP concentration brought about by treatment of cells with the ionophore carbonyl cyanide *p*-trifluoromethoxyphenylhydrazone (FCCP) at 3.5 h poststarvation (PS). FCCP is a proton ionophore that quickly dissipates the proton motive force (pmf) and induces stress responses (Jordan et al., 2008), resulting in a rapid four-fold decrease in the ATP concentration in growing *B. subtilis* (Strahl & Hamoen, 2010). As controls, aliquots from the same cultures were left untreated. The Luc substrate luciferin (which rapidly penetrates into both the MC and the FS, see below) was added to each aliquot and used to measure the luminescence intensity at 3.75 h PS (i.e. 15 min later). In addition, the Luc level was assessed by immunoblot analysis.

For native Luc expressed from the corresponding gene fused to either promoter, neither luminescence intensity (Fig. 2A) nor the protein level (Fig. 2B) changed much after treatment with FCCP (100 μM). We conclude that native Luc was insensitive to any decrease in ATP concentration brought about by the FCCP treatment, presumably because the ATP concentration remained above the relatively low K_m for Mg-ATP (160 μM) of native Luc (Branchini et al., 1999). Insensitivity of native Luc to changes in ATP concentration in growing bacteria has been reported previously (Schneider & Gourse, 2004, Di Tomaso et al.,

2001). Both luminescence intensity (Fig. 2A) and the protein level (Fig. 2B) were less when the gene was expressed from the *spoIIQ* promoter than from the *spoIID* promoter.

In contrast to the situation when using the gene for native Luc, when the gene encoding Luc H245F was expressed from either promoter, luminescence intensity decreased by about sevenfold after FCCP treatment (Fig. 2C). Even without FCCP treatment, luminescence from Luc H245F was much less than from native Luc (Fig. 2A), as expected since Luc H245F has a larger K_m for Mg-ATP and a 16-fold smaller turnover number (k_{cat}) than native Luc (Branchini et al., 1999). The Luc H245F protein levels (Fig. 2D) were only slightly lower than for native Luc (Fig. 2B), and changed little after FCCP addition (Fig. 2D). Importantly, the decreased luminescence intensity from Luc H245F (Fig. 2C) appeared to indicate significantly reduced concentrations of ATP in both the MC and the FS after FCCP treatment.

To measure the effect of FCCP treatment on the cellular ATP concentration during sporulation by an independent method, *B. subtilis* at 3.5 h PS were treated with FCCP (100 μM) or left untreated for 15 min, then boiled to extract ATP. The concentration of ATP in the extracts was determined by comparison with ATP solutions of known concentration (Fig. S1A), using a well-established assay that measures luminescence intensity after mixing with luciferin and firefly lantern extract containing Luc (McElroy, 1947). The ATP concentration decreased more than fivefold after FCCP treatment (Fig. S1B), in approximate agreement with the seven-fold decrease in luminescence intensity after FCCP treatment of strains expressing the gene for Luc H245F from either promoter (Fig. 2C).

Taken together, the results are consistent with the expectation that the K_m for Mg-ATP of Luc H245F is closer than that of native Luc to the cellular ATP concentrations and therefore a more sensitive indicator of changes in the ATP concentration *in vivo*. Hence, all subsequent experiments utilized Luc H245F. Expression of the gene encoding Luc H245F from the σ^E-dependent *spoIID* promoter and the σ^F-dependent *spoIIQ* promoter was expected to confine the protein to the MC and FS, respectively (Sharp & Pogliano, 2002). Since activity of σ^E depends on prior activity of σ^F, a null mutation in *sigF* was expected to prevent expression of the gene encoding Luc H245F from either promoter, whereas a null mutation in *sigE* was expected to prevent expression from the *spoIID* promoter but allow expression from the *spoIIQ* promoter. These expectations were met, based on measuring luminescence intensity of strains bearing the fusions at the *amyE* locus of *sigF* or *sigE* mutants at various times PS (Fig. S2). Therefore, we infer that expression of *luc H245F* from the *spoIID* and *spoIIQ* promoters is indeed confined to the MC and FS, respectively. Altogether, our results support the conclusion that compartment-specific expression of the gene coding for Luc H245F during sporulation allows detection of about a seven-fold decrease in the ATP concentration in both the MC and the FS after FCCP treatment.

Using Luc H245F to measure relative ATP concentrations *in vivo*

For the experiment shown in Figure S2, starvation was initiated in flasks; at 2 h PS, culture aliquots were transferred to a 96-well plate in which luciferin had been added to the wells. Like the flasks, the plate was subjected to vigorous shaking to aerate the samples. Beginning at 2.5 h PS, shaking was stopped briefly to measure luminescence intensity, then shaking

continued until the next measurement. We expected expression of *luc H245F* from the *spoIID* and *spoIIQ* promoters to increase between 1.5 and 2.5 h PS, based on *lacZ* expression from these promoters (Sharp & Pogliano, 2002). We also expected luciferin to rapidly enter *B. subtilis* without addition of a membrane permeabilizing agent (Mirouze et al., 2011), in contrast to *E. coli* (Schneider & Gourse, 2004). However, in the previous experiments with *B. subtilis*, luciferin was added during growth and sporulation was induced upon nutrient exhaustion (Mirouze et al., 2011). Therefore, it was important to determine the effects of adding luciferin at different times PS under our conditions of inducing sporulation by the resuspension method (Sterlini & Mandelstam, 1969). We performed two such experiments, which are described in the Supporting Information. The results suggest that luciferin rapidly enters both the MC and the FS at 2 to 6 h PS, and is not significantly depleted by Luc H245F activity (Fig. S3). Therefore, in the sporulation experiments reported below, starvation was initiated in flasks; at 2 h PS, culture aliquots were transferred to a 96-well plate in which luciferin had been added to the wells.

In agreement with the expectation that expression of *luc H245F* from the *spoIID* and *spoIIQ* promoters would increase between 1.5 and 2.5 h PS (Sharp & Pogliano, 2002), Luc H245F was observed at 2.5 to 6 h (Fig. 3A). In both compartments, the Luc H245F level reached a maximum at 3.5 to 4 h PS, and decreased at later times. One method to account for different levels of Luc H245F at different times is to measure the enzyme level by immunoblot and use this value to normalize the measured luminescence intensity. The normalized luminescence intensity is expected to reflect the cellular ATP concentration, provided Luc H245F is limiting for luminescence. To determine a range over which Luc H245F is limiting for luminescence, we created a strain bearing the IPTG-inducible *hyperspank* promoter fused to *luc H245F* at the *amyE* locus and used it to produce Luc H245F at different levels in parallel growing cultures. We reasoned that such cultures would have a very similar cellular ATP concentration and therefore yield a very similar normalized luminescence intensity over the range in which Luc H245F is limiting for luminescence. The experiments are described in the Supporting Information. The results show that the normalized luminescence intensity (i.e., luminescence intensity/Luc H245F protein level) is very similar over a broad range of Luc H245F levels, indicating that Luc H245F is limiting for luminescence over a broad range in growing cells (Fig. S4). Therefore, both luminescence intensity and the Luc H245F protein level were measured in the experiments described below, and the normalized luminescence intensity is reported as the “relative ATP concentration.”

The available ATP concentration rises nearly twofold in the mother cell during sporulation and does not decline in the forespore

To test for changes in ATP concentration during sporulation, strains expressing *luc H245F* in the MC or FS from the *spoIID* or *spoIIQ* promoter, respectively, were starved to induce sporulation and the luminescence intensities and Luc H245F protein levels were measured at various times PS. The luminescence intensity rose in the MC and in the FS by 3 h and was greater in the MC than in the FS through 6 h (Fig. 3B). We note that luminescence intensities at 2.5 and 3 h were most variable between experiments (e.g. Fig. S3 and 3B), which we attribute to differences in the timing of Luc H245F accumulation. For the

experiment shown in Figure 3B, representative immunoblots show the Luc H245F levels (Fig. 3A) and quantification of biological replicates is shown in Figure 3C. The Luc H245F levels were on average slightly higher in the MC than the FS, and reached maxima at 3.5 h and 4 h, respectively.

The relative ATP concentration (i.e., luminescence intensity/Luc H245F protein level) showed an upward trend in the MC from 3.5 to 6 h PS (Fig. 3D). The increase from 3.5 to 5 h was 1.4-fold on average ($P = 0.031$ in a paired two-tailed *t*-test) and from 3.5 to 6 h was 1.7-fold ($P = 0.033$). These results are consistent with the possibility that loss of channel function upon completion of engulfment allows the MC ATP concentration to rise (Fig. 1, top right).

The relative ATP concentration in the FS also showed an upward trend from 4 to 6 h PS (Fig. 3D). The increase was 1.8-fold on average, but comparison of the data at the two time points using a paired two-tailed *t*-test yielded $P = 0.17$, owing mainly to the large standard deviation of the 6 h samples. Importantly, we did not observe a decline in the FS ATP concentration, which we thought might accompany loss of channel function upon engulfment completion (Fig. 1, top right).

Although a decrease in FS luminescence intensity after FCCP treatment at 3.5 h PS was detected using Luc H245F (Fig. 2C), our results in Figure 3D raised the question of whether Luc H245F remains a sensitive indicator of decreased ATP concentrations at later times. Therefore, the effects of 100 μM FCCP treatment on luminescence intensity and the Luc H245F level were measured to determine the relative ATP concentration after FCCP treatment as a percentage of the untreated control from 4 to 6 h PS. FCCP treatment decreased the ATP concentration to 9-23% that of the untreated control at all times in both compartments (Fig. S5), supporting the use of Luc H245F to measure decreases in ATP concentration in the FS and MC during sporulation.

Since the relative ATP concentration increased nearly twofold on average in both the MC and the FS from 3.5 or 4 h PS to 6 h PS (Fig. 3D), we measured the ATP concentration in extracts of boiled cells at 3.5 and 6 h, expecting an increase at the later time. Instead, we observed a decrease of nearly twofold (Fig. S6). As noted previously, the ATP pool available to Luc H245F *in vivo* may differ from the ATP pool extractable from cells by a particular method (Schneider & Gourse, 2004). Presumably, boiling releases ATP from cellular proteins or other macromolecules, and more accurately reflects the total ATP pool, whereas the ATP pool available to Luc H245F better reflects that available for cellular processes *in vivo*. Under our conditions, <40% of the cells were not sporulating at 3.5 h and <30% were not sporulating at 6 h (data not shown). Presumably, the non-sporulating cells fail to produce Luc H245F and therefore have no effect on the measurement of relative ATP concentrations (Fig. 3D). In contrast, non-sporulating cells contribute to ATP measured by extraction methods, so a decrease in the total ATP pool in non-sporulating cells between 3.5 and 6 h may contribute to the decrease observed in Figure S6. Additional discussion of this experiment and others in which comparisons were made between the relative ATP concentration determined using Luc H245F and the concentration of ATP in cell extracts, can be found in the Supporting Information.

Taken together, our results suggest that the available ATP concentration rises nearly twofold in the MC between 3.5 and 6 h PS, while the concentration of ATP in the FS does not decline. To help interpret these observations, we examined morphological changes and the levels of key sporulation proteins in samples collected during the experiments to measure ATP, as described in the next section.

The rising mother cell ATP concentration correlates with progression of engulfment, cleavage of Pro-σ^K, and decreasing levels of channel proteins

To examine morphological changes during sporulation of the strains used to measure the relative ATP concentration in the MC and the FS, confocal fluorescence microscopy was used to track the progression from formation of flat polar septa to curved septa, through the early stage of engulfment, and finally to the late or complete stage of engulfment (Fig. 4). For simplicity, only the counts for the strain producing Luc H245F in the MC are shown. The strain synthesizing Luc H245F in the FS exhibited no significant difference. The majority of sporangia formed flat or curved septa at 2.5 and 3 h PS. By 3.5 h, most sporangia were at the late stage of engulfment or had completed engulfment. Therefore, progression to the late stage and completion of engulfment occurred with normal timing, which we note correlated with the beginning of the rise in the available ATP concentration in the MC (Fig. 3D).

To examine changes in protein levels during sporulation, samples were subjected to immunoblot analysis. Cleavage of Pro-σ^K was observed at 4.5 h PS and the cleaved σ^K level rose thereafter (Fig. 5, wild-type cells), as expected (Halder et al., 2017). Cleavage of Pro-σ^K requires completion of engulfment, σ^G-dependent expression of *spoIVB*, and relief of inhibition of SpoIVFB protease activity (Kroos & Akiyama, 2013, Konovalova et al., 2014). The levels of SpoIVFA (a negative regulator of SpoIVFB) (Cutting et al., 1991b, Rudner & Losick, 2002) and SpoIVFB decreased at 5 and 6 h (Fig. 5), as expected (Halder et al., 2017). The levels of the channel proteins SpoIIQ and SpoIIIAH peaked at 3 to 3.5 h and decreased thereafter, consistent with reported degradation of channels (Jiang et al., 2005, Chiba et al., 2007, Meisner et al., 2008). We conclude that changes in protein levels during sporulation occurred with normal timing. We note that decreasing levels of channel proteins after 3.5 h (Fig. 5) coincided with the rising MC ATP concentration (Fig. 3D). This correlation is consistent with the possibility that channel destruction upon engulfment completion causes an increase in the MC ATP concentration (Fig. 1, top right). To gain further insight into a possible role of the channels in regulating compartment-specific ATP levels, we next examined the effects of null mutations in genes encoding channel proteins.

Loss of channel proteins has modest and varied effects on the ATP concentration in the mother cell and the forespore

To test whether channel proteins impact the ATP concentration in either compartment during sporulation, null mutations in *spoIIQ, spoIIIAH*, and *spoIIIAA* were transformed into the strains that produce Luc H245F in the MC or FS. We chose these mutations because SpoIIQ and SpoIIIAH form the channel (Blaylock et al., 2004, Doan et al., 2005), and SpoIIIAA ATPase may control substrate transport through the channel on the MC side (Meisner et al., 2008, Doan et al., 2009), whereas the functions of the other SpoIIIA proteins are less well-

defined. To determine the relative ATP concentrations during sporulation, we measured the luminescence intensities and Luc H245F levels of the mutants that synthesize Luc H245F in the MC or FS. Like the WT strains, the luminescence intensities in the mutants were greater in the MC than in the FS by 3 h PS and remained more intense in the MC than in the FS through 6 h (Fig. S7). On average, the maximum luminescence intensity in the MC was slightly greater in the *spoIIQ* mutant and slightly less in the *spoIIIAH* mutant as compared to WT cells and the *spoIIIAA* mutant. The maximum Luc H245F level on average was about two-fold lower in the FS of the *spoIIQ* mutant and in both compartments of the *spoIIIAA* mutant as compared WT cells and the *spoIIIAH* mutant (Fig. S8). The two-fold lower Luc H245F level in the FS of the *spoIIQ* and *spoIIIAA* mutants was unexpected because the FS-specific promoter we used (Londono-Vallejo, 1997) was previously shown to be equally expressed in *spoIIQ* and *spoIIIAA-AH* mutants compared to WT cells using a *lacZ* reporter (Camp & Losick, 2009). The two-fold lower level of Luc H245F in the MC of the *spoIIIAA* mutant was also surprising, since the MC-specific promoter we used (Eichenberger et al., 2004) was previously shown to be equally expressed in *spoIIIA* mutants compared to WT cells using a *lacZ* reporter (Clarke et al., 1986). Perhaps the mutants differ from WT cells in posttranscriptional regulation of Luc H245F levels. In any case, the luminescence intensities and Luc H245F levels were within the usable range established by our control experiments (Fig. S4A and S4D–F).

The relative ATP concentration in the MC was greater on average in the *spoIIQ* and *spoIIIAA* mutants than in WT cells from 3.5 to 5 h PS, and was greater in the *spoIIIAA* mutant than in WT cells at 6 h as well (Fig. 6A). Using Student's two-tailed *t*-tests to compare the data for each mutant with WT cells at the same time PS, $P < 0.05$ was observed at the times indicated by the asterisks ($P < 0.005$ indicated by two asterisks). The results suggest that the MC ATP concentration increases earlier in the *spoIIQ* and *spoIIIAA* mutants than in WT cells, consistent with the hypothesis that functional channels normally decrease the ATP concentration in the MC (Fig. 1, top right). However, the MC ATP concentration did not increase after 3 h in the *spoIIIAH* mutant (Fig. 6A). Rather, the concentration was less on average than in WT cells at all times measured, and $P < 0.05$ was observed at 4.5 to 6 h owing to the increase seen in WT cells. Thus, the loss of channel proteins had modest effects on the MC ATP concentration, differing from WT cells by less than twofold on average, and the effects varied for loss of different channel proteins.

The FS ATP concentration in the *spoIIIAH* mutant was less on average than in WT cells at all times, and $P < 0.05$ was observed at 3 h and thereafter (Fig. 6B). However, the FS ATP concentration in the *spoIIQ* mutant was similar to that of WT cells, as was that of the *spoIIIAA* mutant at 4 h and thereafter (i.e. $P > 0.05$), suggesting that a low ATP level does not explain the lack of post-engulfment FS gene expression in the *spoIIQ* and *spoIIIAA* mutants (see Discussion). We conclude that the loss of channel proteins had modest effects on the FS ATP concentration, differing from WT cells by less than twofold on average, with the exception that loss of SpoIIIAH lowered the concentration more than twofold relative to WT cells at 4.5 h and thereafter. We considered the possibility that SpoIIQ allows leakage of ATP from the FS of the *spoIIIAH* mutant and the *spoIIIAA* mutant at 3 and 3.5 h, due to impaired channel assembly/activity. However, we found that the *spoIIQ* mutation did not

restore the FS ATP concentration in either the *spoIIIAA* or the *spoIIIAH* mutant background (Fig. S9).

We characterized the membrane morphology of the *spoIIQ, spoIIIAH*, and *spoIIIAA* single mutants. The *spoIIQ* and *spoIIIAH* mutants were impaired for engulfment. Unlike WT cellls, the majority of mutant sporangia were in the early stage of engulfment when examined at 6 h PS (Table 1). Approximately half of the sporangia that had advanced farther, to the late stage or completion of engulfment, exhibited a FS that appeared to be smaller than usual or misshapen, as reported previously (Doan et al., 2009). Additionally, a few disporic cells (i.e. cells with a FS compartment at each end) were observed. The partial defect in engulfment at 6 h was unexpected, since *spoIIQ* and *spoIIIAH* mutants have been reported to exhibit only modest delays in completion of engulfment (Broder & Pogliano, 2006, Londono-Vallejo et al., 1997, Sun et al., 2000). However, SpoIIQ and SpoIIIAH are essential for engulfment under certain conditions (Broder & Pogliano, 2006, Sun et al., 2000), and apparently the two proteins play an important role in engulfment under our conditions, which included transfer to 96-well plates at 2 h. We note the possibility that partial defects in engulfment could impact compartment-specific ATP levels. In contrast, the *spoIIIAA* mutant strains (i.e. the two strains with the same *spoIIIAA* mutation, but expressing *luc H245F* in the MC or FS) were similar to WT cells at 6 h (Table 1). However, as expected, at 24 h the efficiency of heat-resistant spore formation by the *spoIIIAA* mutants was 0.01% that of WT cells.

We also characterized the mutants with respect to protein levels using immunoblot analysis as for WT cells. The levels of SpoIVFA and SpoIVFB were similar to those in WT cells, albeit with slightly less SpoIVFA in the *spoIIQ* and *spoIIIAA* mutants (Fig. 5). Also, in all three mutants, the SpoIVFB level was higher than in WT cells at 6 h PS, presumably because sporulation was blocked. As expected (Jiang et al., 2005), no σ^K was observed in the *spoIIQ* and *spoIIIAA* mutants (Fig. 5). A very small amount of σ^K was seen in the two *spoIIIAH* mutant strains (engineered to express *luc H245F* in the MC or FS), consistent with the observations that *spoIIIAH* mutants form heat-resistant spores with higher efficiency than other *spoIIIA* mutants (Doan et al., 2009) because SpoIIIAH and GerM are partially redundant in function (Rodrigues et al., 2016b). The level of SpoIIIAH was lower in the *spoIIQ* mutant than in WT cells, and accumulation of SpoIIIAH was delayed by about 30 min in the *spoIIQ* and *spoIIIAA* mutants (Fig. 5). The level of SpoIIQ was lower in the *spoIIIAA* and *spoIIIAH* mutants than in WT cells, although the temporal pattern of accumulation was similar.

In sum, our results provide evidence that loss of channel proteins has modest and varied effects on the ATP concentration in both the MC and the FS, and that loss of one channel protein can influence the level of other channel proteins.

Channel proteins persist in a *spoIVB* mutant and the ATP concentration remains low in the mother cell and the forespore

Since SpoIVB is a protease that cleaves SpoIIQ (Chiba et al., 2007), we reasoned that channels may not be degraded normally in a *spoIVB* mutant, perhaps impacting compartment-specific ATP levels. To test this hypothesis, a null mutation in *spoIVB* was

transformed into the strains that produce Luc H245F in the MC or FS. Indeed, the channel proteins SpoIIQ and SpoIIIAH persisted in the *spoIVB* mutant strains at least until 6 h PS (Fig. 7A), unlike in WT cells (Fig. 5). As expected, Pro-σ^K remained uncleaved in the *spoIVB* mutant strains (Fig. 7A), since SpoIVB is required to relieve inhibition of SpoIVFB (Cutting et al., 1991a, Wakeley et al., 2000, Zhou & Kroos, 2005, Campo & Rudner, 2006, Campo & Rudner, 2007). To determine the relative ATP concentrations during sporulation, we measured the luminescence intensities and Luc H245F levels of the *spoIVB* mutant strains. In both compartments, the luminescence was more intense at 2.5 h as compared to WT cells, but comparable at later times (Fig. S7). At all times, the Luc H245F level in the MC of the *spoIVB* mutant was higher than in the MC of WT cells (Fig. S8), but the levels were within the usable range established by our control experiments (Fig. S4A and S4D–F). Importantly, the relative ATP concentration remains low in both compartments during sporulation (Fig. 7B). The failure of the ATP level to increase in the MC of the *spoIVB* mutant is consistent with the notion that channel destruction upon engulfment completion in WT cells causes the MC ATP concentration to increase (Fig. 1, top right). The FS ATP concentration in the *spoIVB* mutant was less on average than in WT cells at all times after 2.5 h, and $P < 0.05$ was observed at 3.5 to 4.5 h (Fig. 7B).

Bypass mutants lacking channel proteins do not accumulate more σ^K than a bypass mutant with channel proteins

The *spoIIQ*, *spoIIIAH*, and *spoIIIAA* mutants exhibited little or no accumulation of σ^K (Fig. 5), as expected since these mutants fail to activate σ^G in the FS (Blaylock et al., 2004, Doan et al., 2005, Camp & Losick, 2008, Meisner et al., 2008, Camp & Losick, 2009, Doan et al., 2009). Activity of σ^G is necessary to relieve inhibition of SpoIVFB by SpoIVFA and BofA, allowing cleavage of Pro-σ^K (Cutting et al., 1991a, Zhou & Kroos, 2005, Campo & Rudner, 2006, Cutting et al., 1990, Rudner & Losick, 2002, Zhou & Kroos, 2004, Ramirez-Guadiana et al., 2018). However, the dependence of Pro-σ^K cleavage on σ^G activity can be bypassed by mutations in *spoIVFA* or *bofA* (Cutting et al., 1990, Cutting et al., 1991b, Ricca et al., 1992). We reasoned that a bypass mutation in combination with a null mutation in *spoIIQ* or *spoIIIAA* might result in earlier and/or elevated accumulation of σ^K, because *spoIIQ* and *spoIIIAA* mutations increased the MC ATP concentration relative to WT cells (Fig. 6A), and the CBS domain of SpoIVFB may sense the MC ATP concentration and stimulate Pro-σ^K cleavage (Halder et al., 2017, Zhou et al., 2009). We combined the *bofB8* bypass mutation in *spoIVFA* with null mutations in *spoIIQ*, *spoIIIAH*, and *spoIIIAA*. All strains with the *bofB8* mutation also have a null mutation in *sigG*, which codes for σ^G (Karmazyn-Campelli et al., 1989). The *sigG* mutation blocks *spoIVB* expression (Cutting et al., 1991a), but the *bofB8* mutation bypasses the need for SpoIVB to relieve inhibition of SpoIVFB (Cutting et al., 1990). We measured the Pro-σ^K and σ^K levels during sporulation. As expected (Cutting et al., 1990), the *bofB8* mutation advanced the timing of accumulation of σ^K, but in combination with the other mutations, σ^K accumulation was barely detectable (*spoIIQ*), reduced (*spoIIIAH*), or similar to *bofB8* alone (*spoIIIAA*) (Fig. 8A). Hence, mutants lacking channel proteins did not accumulate σ^K earlier or at an elevated level. These results suggest that the MC ATP concentration is not limiting for SpoIVFB cleavage of Pro-σ^K under these conditions. Below, we consider two other factors that may have limited SpoIVFB cleavage of Pro-σ^K in this experiment.

First, we examined accumulation of SpoIVFB, because previously a bypass mutation (*bofA*Δ) in combination with a null mutation in *spoIIQ* was shown to greatly reduce SpoIVFB accumulation and σ^K was undetectable during sporulation (Doan & Rudner, 2007). In contrast to the *bofA*Δ mutation, the *bofB8* mutation in combination with a null mutation in *spoIIQ* did not impair SpoIVFB accumulation, as compared with the *bofB8* mutation alone (Fig. 8A). SpoIVFB accumulation was also similar for the *bofB8* mutation in combination with a null mutation in *spoIIIAH* or *spoIIIAA.*

Since SpoIVFB accumulated, we considered the possibility that it was mislocalized. Previously, null mutations in *spoIIQ* or *spoIIIAH-G* (i.e. deletion of both *spoIIIAG* and *spoIIIAH*) were reported to prevent localization of SpoIVFB-GFP to the engulfing membrane, although SpoIVFB-GFP appeared to accumulate in the outer FS membrane after completion of engulfment (Jiang et al., 2005). We created strains in which the native *spoIVFB* gene was C-terminally fused to *gfp*, resulting in production of a functional SpoIVFB-GFP fusion protein (Rudner & Losick, 2002). Immunoblot analysis of all the strains with antibodies against GFP revealed that SpoIVFB-GFP migrated at the expected position, with very little or no free GFP due to degradation (Fig. S10). Therefore, we examined SpoIVFB-GFP localization using confocal fluorescence microscopy. The *bofB8* mutation alone or in combination with the null mutation in *spoIIIAA*, allowed predominantly FS localization of SpoIVFB-GFP (presumably to the outer FS membrane) (Fig. 8B), consistent with their similar σ^K accumulation (Fig. 8A). In contrast, the *bofB8* mutation in combination with a null mutation in *spoIIQ* or *spoIIIAH* resulted in considerable MC fluorescence in most sporangia (Fig. 8B), suggesting that SpoIVFB-GFP was predominantly mislocalized, which may explain why σ^K accumulation was impaired (Fig. 8A).

We conclude that SpoIIIAA is not required for proper localization of SpoIVFB-GFP or for normal accumulation of SpoIVFB in the context of the *bofB8* bypass mutation (Fig. 8). Yet, loss of SpoIIIAA does not elevate σ^K accumulation in the bypass mutant (Fig. 8A), even though loss of SpoIIIAA does elevate the MC ATP concentration relative to WT cells (Fig. 6A). Together, these results strongly suggest that the MC ATP concentration is not limiting for SpoIVFB cleavage of Pro-σ^K under these conditions. Moreover, in the strains with the *bofB8* mutation alone or in combination with the *spoIIIAA* mutation, σ^K accumulates as soon as Pro-σ^K is detected (Fig. 8A), suggesting that the MC ATP concentration is sufficient for SpoIVFB cleavage of Pro-σ^K before the ATP concentration rises in the MC (Fig. 3D). Hence, even though SpoIVB-dependent channel destruction upon engulfment completion may cause the MC ATP level to rise (Fig. 7) as hypothesized (Fig. 1, top right), the rise does not appear to be necessary for SpoIVFB to cleave Pro-σ^K (Fig. 8A).

Both ionophores and chloramphenicol decrease the mother cell ATP concentration, yet Pro-σ^K can be cleaved

Since SpoIVFB did not appear to sense the rise in the MC ATP concentration, we tested whether SpoIVFB would be inhibited by a decrease in ATP concentration brought about by treatment with an ionophore. In a previous study, the ionophore carbonyl cyanide *m*-chlorophenylhydrazone (CCCP) was shown to inhibit cleavage of Pro-σ^K during *B. subtilis*

sporulation, but the inhibition appeared to be primarily due to decreased synthesis of SpoIVB (Kroos et al., 2002). SpoIVB cleaves the extracytoplasmic domain of SpoIVFA in the space between the membranes surrounding the FS, relieving inhibition of SpoIVFB (Wakeley et al., 2000, Zhou & Kroos, 2005, Campo & Rudner, 2006, Ramirez-Guadiana et al., 2018). The *spoIVB* gene is transcribed by σ^G RNA polymerase (Cutting et al., 1991a), which is the primary reason that σ^G activity is required for Pro-σ^K cleavage (Cutting et al., 1990). Using the same *bofB8 sigG* bypass mutant as in the experiments shown in Figure 8, the inhibition of Pro-σ^K cleavage by CCCP (5 μM) was partially overcome (Kroos et al., 2002). This raised the question whether 5 μM CCCP treatment substantially lowered the ATP level in the MC during *B. subtilis* sporulation. Therefore, we compared the effects of different ionophores at different concentrations on the relative ATP concentration in the MC.

We compared the effects of CCCP and FCCP treatments at 5 and 100 μM at 3.5 h PS. As observed for treatment with 100 μM FCCP (Fig. 2C and 2D), the other treatments primarily decreased the luminescence intensity (Fig. S11A) and had little impact on the Luc H245F level (Fig. S11B), resulting in normalized values that indicate all four treatments decreased the relative ATP concentration in the MC after 15 min (Fig. 9A). The decrease brought about by 5 μM CCCP (~57%) was less than for 5 μM FCCP (~71%), and 100 μM CCCP (~81%) or FCCP (~94%) caused larger decreases.

Since treatment with ionophores decreased the relative ATP concentration in the MC, we tested whether cleavage of Pro-σ^K by SpoIVFB was inhibited by ionophores. We used the same *bofB8 sigG* bypass mutant as in the experiments shown in Figure 8 and in the previous study (Kroos et al., 2002). As explained above, the *bofB8* mutation bypasses the need for σ^G-dependent expression of *spoIVB*, which normally is required to relieve inhibition of SpoIVFB and allow Pro-σ^K cleavage (Cutting et al., 1990, Cutting et al., 1991b, Cutting et al., 1991a). We anticipated that ionophores would inhibit protein synthesis (Kroos et al., 2002), so it was necessary to bypass the need for synthesis of SpoIVB. As a control, we tested the effect of the protein synthesis inhibitor chloramphenicol (Cm) on Pro-σ^K cleavage in the bypass mutant, expecting to observe cleavage based on the previous study (Kroos et al., 2002). In the bypass mutant at 2.5 h PS, Pro-σ^K is more abundant than σ^K (Fig. 9B, lane 1), but by 3 h, σ^K is more abundant (lane 2), due to cleavage of Pro-σ^K by SpoIVFB (the σ^K/Pro-σ^K ratio is shown below each lane). Treatment at 2.5 h with CCCP or FCCP at 5 or 100 μM partially inhibited Pro-σ^K cleavage by 3 h (lanes 3-6) since the σ^K/Pro-σ^K ratio did not increase as much as in lane 2, although it did increase a little in comparison with lane 1. The ionophores also partially inhibited Pro-σ^K synthesis, as the combined accumulation of Pro-σ^K and σ^K in lanes 3-6 was less than in lane 2, but more than in lane 1 (Table S1). In contrast, treatment with Cm did not inhibit Pro-σ^K cleavage (Fig. 9B, lane 7), although it blocked further synthesis of Pro-σ^K (Table S1). The abundance of SpoIVFB was similar at 2.5 h and at 3 h under all conditions (Fig. 9B, bottom panel). Because ionophores and Cm had different effects on Pro-σ^K cleavage, we next investigated whether Cm affects the MC ATP concentration.

We did not expect Cm treatment to decrease the MC ATP concentration, since Cm treatment of growing *E. coli* cells increased the relative ATP concentration about twofold after 10 min, presumably since less ATP was being utilized for protein synthesis (Schneider & Gourse,

2004). However, we found that Cm, like the ionophores, decreases the luminescence intensity by 15 min after treatment and has little effect on the Luc H245F level, hence decreasing the relative MC ATP concentration (Fig. S12). The decrease (53%) was comparable to that caused by 5 μM CCCP (57%) (Fig. 9A) and less than that by 100 μM FCCP (73%) in the same experiment (Fig. S12). We note that the decrease by 100 μM FCCP varied somewhat in different experiments (94% in Fig. 9A), but was consistently greater than that by Cm or 5 μM CCCP. Since treatments with Cm or 5 μM CCCP led to similar decreases in the MC ATP level after 15 min (Fig. 9A and S12C) but appeared to have different effects on Pro-σ^K cleavage after 30 min (Fig. 9B), we next compared the treatments more carefully in time course experiments.

We reasoned that the 5 μM CCCP treatment might cause the MC ATP concentration to decrease more rapidly than the Cm treatment, explaining the partial inhibition of Pro-σ^K cleavage by CCCP and the lack of cleavage inhibition by Cm (Fig. 9B). The treatments were performed at 2.5 h to match the time of treatments in the experiment shown in Figure 9B. We found that Cm caused the MC ATP concentration to decrease at least as rapidly as CCCP (Fig. 9C and S13). Hence, these results do not explain the different effects of the two treatments on Pro-σ^K cleavage (Fig. 9B). Since ionophores induce stress responses (Jordan et al., 2008), the resulting pleiotropic effects on cellular physiology may inhibit Pro-σ^K cleavage more than treatment with Cm.

Because Cm blocked further Pro-σ^K synthesis (Table S1), yet allowed cleavage to σ^K after 30 min (Fig. 9B, lane 7), we repeated the experiment shown in Figure 9B in order to examine the time course of Pro-σ^K cleavage. Without treatment at 2.5 h PS, the σ^K level increased slightly after 5 min, markedly after 15 min, and overtook Pro-σ^K in abundance after 30 min (Fig. 9D, lanes 1-4). Treatment with 5 μM CCCP inhibited Pro-σ^K cleavage as reflected by the σ^K/Pro-σ^K ratio (lanes 5-7). The ratio did not increase after 30 min (lane 7), as it had in the experiment shown in Figure 9B (lane 3), indicating that cleavage inhibition varied slightly between experiments. In both experiments, 5 μM CCCP partially inhibited Pro-σ^K synthesis as reflected by the combined accumulation of Pro-σ^K and σ^K (Table S1; compare lanes 5-7 with lanes 2-4 for the experiment shown in Fig. 9D). A small amount of σ^K and a larger amount of Pro-σ^K accumulated steadily by 30 min after CCCP treatment (Fig. 9D, lanes 5-7; Table S1). The increase in the level of σ^K suggests that Pro-σ^K continued to be cleaved as the MC ATP concentration declined (Fig. 9C). Treatment with Cm blocked further Pro-σ^K synthesis, yet the σ^K/Pro-σ^K ratio increased (Fig. 9D, lanes 8-10; Table S1), suggesting that Pro-σ^K cleavage continued as the MC ATP concentration declined (Fig. 9C). These results strongly suggest that a low level of ATP in the MC can support ongoing cleavage of Pro-σ^K, strengthening our conclusion that a rise in the MC ATP level is not necessary for SpoIVFB to cleave Pro-σ^K (Fig. 8A).

Discussion

We devised a method to measure the relative ATP concentration in each compartment during sporulation and used the method to show that the ATP concentration rises nearly twofold in the MC coincident with progression of engulfment, and decreasing levels of channel proteins. The coincidence of these events is consistent with a model in which engulfment

completion and ensuing channel destruction cause the MC ATP concentration to rise (Fig. 1, top right). The failure of the ATP level to rise in the MC of a *spoIVB* mutant in which channel proteins persist is also consistent with the model. However, the rise in MC ATP concentration is not necessary for Pro-σ^K cleavage, based on our analysis of mutants that bypass the normal requirement for the σ^G-dependent signaling pathway from the FS to relieve inhibition of SpoIVFB.

Although the model predicted a decrease in the FS ATP concentration after engulfment completion (Fig. 1, top right), we did not observe a decline by 6 h PS, even though the majority of Pro-σ^K had been cleaved to σ^K by that time, indicating that engulfment was complete and σ^G had become active. Since expression of the σ^G regulon consumes ATP, our findings suggest that ATP must be generated in the FS post-engulfment. Because treatment with a proton ionophore rapidly decreased the FS ATP concentration at 6 h PS, a pmf across the inner FS membrane may drive ATP synthesis after channel destruction. Importantly, the SpoIIQ and SpoIIIAA channel proteins were not required to maintain the normal FS ATP concentration at 4 h PS and thereafter, yet post-engulfment FS gene expression fails in *spoIIQ* and *spoIIIAA* mutants, suggesting that a factor other than ATP is lacking.

A limitation of using Luc H245F is the inability to observe individual cells microscopically because light production is too low. In an effort to measure relative changes in ATP concentration at single-cell resolution, we attempted expression of a codon-optimized variant of the FRET-based ATP sensor AT1.03 (Imamura et al., 2009) in *B. subtilis*. However, we were unable to generate a strain with sufficient expression to allow measurements (see the Supporting Information).

Channel destruction upon engulfment completion correlates with a nearly two-fold rise in the mother cell ATP concentration, but this is not necessary for Pro-σ^K cleavage

The findings that SpoIVFB has an ATP-binding CBS domain and that cleavage of Pro-σ^K by SpoIVFB *in vitro* depends on ATP led to the suggestion that the SpoIVFB CBS domain senses the MC ATP concentration and regulates Pro-σ^K cleavage appropriately (Zhou et al., 2009). In particular, it was attractive to propose that channel destruction upon completion of engulfment (Chiba et al., 2007, Meisner et al., 2008, Doan et al., 2009) causes the MC ATP concentration to increase and that this change is sensed by the CBS domain of SpoIVFB, triggering cleavage of Pro-σ^K (Konovalova et al., 2014, Kroos & Akiyama, 2013). Several of our findings are consistent with the hypothesis that channel destruction upon engulfment completion causes a rise in the MC ATP concentration, but our data do not support the notion that the SpoIVFB CBS domain senses the increase in the MC ATP level and triggers Pro-σ^K cleavage.

While our findings are consistent with the hypothesis that SpoIVB-dependent channel destruction upon engulfment completion causes the MC ATP level to rise, we cannot rule out other interpretations. For example, the increase in ATP concentration in WT cells (Fig. 3D) could reflect an increase in the available ATP pool as the MC switches from expression of the larger σ^E regulon to the smaller σ^K regulon (Eichenberger et al., 2004, Arrieta-Ortiz et al., 2015). The absence of the rise in the *spoIVB* mutant could be due to its failure to produce σ^K (Fig. 7), whose activity normally initiates feedback loops that negatively

regulate the σ^E regulon (Wang et al., 2007, Zhang & Kroos, 1997, Zhang et al., 1999, Serrano et al., 2015). However, two of the channel protein mutants we tested also fail to produce σ^K (Fig. 5, *spoIIQ* and *spoIIIAA*), yet the relative ATP concentration increased earlier in the MC of these mutants than in WT cells (Fig. 6A). Interestingly, the MC ATP concentration plateaued in the *spoIIQ* mutant, but continued to rise in the *spoIIIAA* mutant until 6 h. This difference may reflect different roles of SpoIIQ and SpoIIIAA in channel function after 4 h. In the absence of SpoIIQ, the SpoIIIAH (Blaylock et al., 2004), SpoIIIAG (Doan et al., 2009), and GerM (Rodrigues et al., 2016b) proteins mislocalize to the MC membrane. Perhaps the SpoIIIA and GerM proteins eventually assemble to some extent in the MC membrane, preventing the ATP concentration from continuing to rise after 4 h in the *spoIIQ* mutant. In the absence of SpoIIIAA, channels may assemble but completely fail to function due to the lack of SpoIIIAA ATPase activity (Doan et al., 2009), so the ATP concentration continues to rise after 4 h in the *spoIIIAA* mutant. In the absence of SpoIIIAH, the MC ATP concentration remained low (Fig. 6A). Since SpoIIIAH and GerM are partially redundant in function (Rodrigues et al., 2016b), channels may assemble but function aberrantly, so the ATP concentration never rises in the *spoIIIAH* mutant.

Our data do not support the notion that the CBS domain of SpoIVFB senses the rise in the MC ATP concentration (Fig. 3D) and triggers Pro-σ^K cleavage (Fig. 5, wild-type cells), although the timing of these events correlates fairly well. Rather, relief from inhibition by SpoIVFA and BofA appears to be sufficient to allow SpoIVFB to cleave Pro-σ^K before the rise in MC ATP concentration. We found that σ^K accumulates as soon as Pro-σ^K is detected in a *bofB8* mutant, by 2.75 h PS (Fig. 8A), well before the rise in MC ATP concentration at 5 to 6 h in WT cells (Fig. 3D). Also, the ratio of σ^K to Pro-σ^K was not larger in the *bofB8 spoIIIAA* double mutant than in the *bofB8* single mutant (Fig. 8A), although the MC ATP concentration was expected to be greater in the double mutant, based on the elevated concentration in the *spoIIIAA* mutant compared to WT cells at 3 and 4 h (Fig. 6A). These observations suggest that the concentration of ATP in the MC is sufficient for SpoIVFB activity prior to the increase that accompanies engulfment completion and channel destruction. In agreement, treatment with ionophores or Cm did not completely block Pro-σ^K cleavage, despite lowering the relative MC ATP concentration to ~0.01 (Fig. 9), which is at least two-fold lower than that present before the increase (Fig. 3D). It is possible that the ionophore and Cm treatments did not lower the ATP level enough to block Pro-σ^K cleavage. However, our findings challenge the suggestion that the SpoIVFB CBS domain senses the MC ATP concentration and regulates Pro-σ^K cleavage appropriately (Zhou et al., 2009). Since the energy status is often sensed as a ratio of adenine nucleotides (Scott et al., 2004), perhaps the SpoIVFB CBS domain senses the ratio of ATP to ADP and/or AMP in the MC. Alternatively, binding of ATP to the SpoIVFB CBS domain may impact oligomerization (Zhou et al., 2009), stability, and/or interactions with other proteins. In any case, YFP can substitute for the CBS domain, producing a partially functional SpoIVFB-YFP fusion protein sufficient for sporulation (Ramirez-Guadiana et al., 2018).

The available ATP concentration in the forespore does not decline despite σ^G activity

Our results suggest that the available ATP concentration is maintained in the FS at least until 6 h PS (Fig. 3D), well after 3.5 h when many sporangia have reached the late stage of

engulfment or have completed engulfment (Fig. 4), and σ^G activity in the FS has led to efficient Pro-σ^K cleavage in the MC and a decrease of channel proteins (Fig. 5, wild-type cells). We infer that σ^G activity does not rapidly deplete the available ATP in the FS after completion of engulfment. Our results suggest that a pmf across the inner FS membrane drives ATP synthesis in the FS after engulfment completion and channel destruction, since treatment with a proton ionophore at 6 h dramatically lowered the relative FS ATP concentration (Fig. S5). This result also indicates that FS ATP is being utilized at 6 h. Presumably, expression of the σ^G regulon accounts for some of the ATP utilization in the FS.

How could a pmf be established across the inner FS membrane after engulfment completion and channel destruction? One possibility is that the MC fuels respiratory chain activity in the outer FS membrane that increases the proton concentration of the intermembrane space and establishes a pmf across both FS membranes. Alternatively, perhaps reserves in the FS generate a pmf across the inner FS membrane. Biochemical analysis of *Bacillus megaterium* forespores has shown that several metabolites (3-phosphoglycerate, arginine, glutamate) accumulate in forespores by 3 h PS (the earliest they could be isolated) or shortly thereafter (Singh et al., 1977). Enzymes for 3-phosphoglycerate utilization are present (Singh et al., 1977), perhaps accounting for some ATP synthesis, but 3-phosphoglycerate continues to accumulate for later utilization during spore germination (Setlow & Kornberg, 1970). In forespores, the 3-phosphoglycerate is not expected to feed into the citric acid cycle since several enzymes are low or absent (Singh et al., 1977), so reduced substrates like NAD(P)H would not be generated. In contrast, catabolism of arginine and/or glutamate could produce NAD(P)H for respiratory chain activity to generate a pmf and ATP synthesis. This hypothesis is based on studies of *B. megaterium* forespores and will need to be tested by analyzing *B. subtilis* forespores.

ATP does not appear to be the limiting factor for post-engulfment forespore gene expression

The FS ATP level on average was lower in the absence of SpoIIIAH than in the absence of SpoIIIAA (Fig. 6B). In a *spoIIIAA* mutant, the initial localization of SpoIIIAH to the polar septum is delayed (Blaylock et al., 2004). Perhaps this finding accounts for the low FS ATP level in the *spoIIIAA* mutant at 3.5 h PS (Fig. 6B). Later during sporulation, proper localization of SpoIIIAH in the *spoIIIAA* mutant may allow the FS ATP level to recover. The FS ATP level was comparable to WT cells in the *spoIIQ* single mutant, at least until 4.5 h (Fig. 6B). The requirement for SpoIIIAH but not SpoIIQ to achieve the normal FS ATP level at 3.5 to 4.5 h indicates that complete channels do not mediate this effect. Rather, we speculate that the absence of SpoIIIAH alters the composition of the intermembrane space in a way that lowers the FS ATP level, and delayed SpoIIIAH localization in the *spoIIIAA* mutant likewise temporarily lowers the FS ATP level.

At 5 and 6 h PS, the FS ATP level was on average slightly lower in the *spoIIQ*, *spoIIIAA*, and *spoIVB* mutants than in WT cells, but paired two-tailed *t*-tests yielded $P > 0.05$ (Fig. 6B and 7B). Although we cannot rule out the possibility that ATP is the limiting factor for post-engulfment FS gene expression in the *spoIIQ* and *spoIIIAA* mutants, this seems very

unlikely since σ^G-dependent genes are expressed in the FS of the *spoIVB* mutant (Cutting et al., 1991a). Why then does σ^G fail to become fully active in *spoIIQ* and *spoIIIA* mutants? The transmembrane segment of SpoIIQ regulates expression of the gene for the anti-σ^G factor CsfB (Flanagan et al., 2016) and several features of the *sigG* promoter, mRNA leader sequence, and start codon dampen expression (Mearls et al., 2018), but these findings do not explain a more general requirement of SpoIIQ and SpoIIIA proteins for macromolecular synthesis in the FS (Camp & Losick, 2009). Our data do not distinguish between models for channel function that propose transport of small molecules (Doan et al., 2009) or a protein (Camp & Losick, 2008, Meisner et al., 2008), or propose a structural role (Rodrigues et al., 2016a). Interestingly, it was suggested that amino acids for protein synthesis in the FS would be obtained from the MC because key amino acid biosynthetic enzymes are low or absent in *B. megaterium* forespores (Singh et al., 1977) and/or mature spores (Setlow & Primus, 1975). Perhaps in WT cells the channels transport amino acids from the MC into the FS during engulfment, and the amino acids are both used directly in protein synthesis and catabolized to maintain the FS ATP concentration after the completion of engulfment as discussed above.

Experimental procedures

Bacterial strains, plasmids, primers, and sporulation—Strains, plasmids, and primers used in this study are listed in Table S2. Genes cloned after PCR or subjected to site-directed mutagenesis were verified by DNA sequencing. *B. subtilis* strains were derived from the WT strain PY79, the *bofB8 sigG* mutant SC777, or the *sigE* mutant AG185 (derived from strain 168). Plasmids for compartment-specific expression of the genes for Luc and Luc H245F were transformed *via* natural competence using the 'Gröningen method' (Bron, 1990) and selecting for chloramphenicol resistance (5 μg/mL). Gene replacements at *amyE* were identified by loss of amylase activity on 1% potato starch medium with Gram's iodine solution (Shimotsu & Henner, 1986). The resulting strains were then transformed (using the Gröningen method) with chromosomal DNA to introduce a mutation in *spoIIQ, spoIIIAA*, or *spoIIIAH* by selecting for genetically linked phleomycin resistance (0.5 μg/mL) and screening for a sporulation defect on DSM (Harwood & Cutting, 1990) containing 1.5% agar. Sporulation was induced by the resuspension method (Sterlini & Mandelstam, 1969), initially in flasks with shaking (400 rpm) at 37°C. Each culture contained approximately the same number of cells, based on an optical density of ~70 Klett units at the time of resuspension to initiate starvation. In some experiments culture aliquots were transferred to 96-well plates as described below, and vigorous shaking (orbital, high setting) at 37°C was continued using a Filtermax F5 plate reader (Molecular Devices). Shaking was interrupted only to measure luminescence intensity and collect samples.

Treatment of cultures with ionophores or chloramphenicol during sporulation—For experiments in which luminescence intensity was measured, sporulation was induced in flasks and at 3.5 h PS culture aliquots (200 μL) were transferred to a 96-well plate (black walls, clear bottom) containing D-luciferin (4.5 mM final concentration), a concentration 300-fold higher than the K_m for luciferin of native Luc and 50-fold higher than that of Luc H245F (Branchini et al., 1999). For each strain, aliquots were either treated with ionophores or chloramphenicol as indicated, or left untreated as a control. Luminescence intensity was

measured using the Filtermax F5 plate reader mentioned above, then the samples were centrifuged at 14,100 × *g* for 3 min, the supernatants were removed, and the cell pellets were stored at −80°C for subsequent immunoblot analysis with anti-Luc antibodies. For experiments in which the relative ATP concentration was determined, each Luc H245F signal was quantified and normalized to a control sample on the same blot, as described below. The luminescence intensity was divided by the Luc H245F protein level to yield a normalized value representing the relative ATP concentration.

In related experiments, sporulation was induced in flasks and at the indicated time the culture was split and subcultures in flasks were treated with ionophores or chloramphenicol as indicated, or left untreated as a control, and then samples were centrifuged, supernatants were removed, and cell pellets were stored at −80°C for subsequent ATP assays of cell extracts (Fig. S1) or immunoblot analyses with anti-Pro-σ^K and anti-SpoIVFB antibodies (Fig. 9B and 9D).

Immunoblot analysis—Whole-cell extracts of *B. subtilis* were prepared as described previously for *E. coli* (Zhou & Kroos, 2004), except 25 μL each of lysis buffer and 2× sample buffer was used for cell pellets from 200 μL samples collected from 96-well plates, and samples were incubated at 55°C for 5 min rather than boiling for 3 min. For experiments in which samples were collected from flasks rather than from 96-well plates (Fig. 8A, 9B, 9D, S10, and S14B), equivalent amounts of cells based on the optical density at 600 nm of the culture were collected from 0.5-1.0 mL by centrifugation at 14,100 × *g* for 3 min, the supernatants were removed, and the pellets were stored at −80°C. Whole-cell extracts were prepared as described above, except using 50 μL each of lysis buffer and 2× sample buffer. Proteins in equal volumes of samples were separated by SDS-PAGE using 14% Prosieve-50 (Lonza) polyacrylamide gels and electroblotted to Immobilon-P membranes (Millipore). Blots were blocked with 5% nonfat dry milk in TBST (20 mM Tris-HCl [pH 7.5], 0.5 M NaCl, 0.1% Tween) for 1 h at 25°C with shaking. Blots were probed with goat anti-Luc horseradish peroxidase (HRP) conjugate (1:10,000) (Rockland catalog #200-103-150-0100) or antibodies against SpoIVFA (1:3000) (Kroos et al., 2002), SpoIVFB (1:5000) (Halder et al., 2017), Pro-σ^K (1:3000) (Lu et al., 1990), SpoIIQ (1:10,000) (Doan & Rudner, 2007), SpoIIIAH (1:10,000) (Campo et al., 2008), or GFP (1:10,000) (Kroos et al., 2002) diluted in TBST with 1% milk and incubated overnight at 4°C with shaking. Antibodies not conjugated to HRP were detected with a goat anti-rabbit-HRP antibody (1:10,000) (Bio-Rad catalog #170-6515) diluted in TBST with 1% milk for 1 h at 25°C with shaking. Signals were generated using the Western Lightning Plus ECL reagent (PerkinElmer) and signals were detected using a ChemiDoc MP imaging system (Bio-Rad), with exposure times short enough to ensure that signals were not saturated. Signal intensities were quantified using Image Lab 5.1 software (Bio-Rad) volume tools.

For experiments in which the relative ATP concentration was determined, each Luc H245F signal was quantified and normalized to a control sample on the same blot. To prepare the control sample, *B. subtilis* strain BDP85, engineered to express *luc H245F* in the MC, was starved to induce sporulation. At 3.5 h PS, cells were collected by centrifugation and a whole-cell extract was prepared as described above for samples collected from flasks, except the whole-cell extracts from several pellets were combined. The resulting control sample

was subjected to SDS-PAGE and immunoblot analysis in parallel with other samples containing Luc H245F. The signal intensity of the other samples was normalized to the signal intensity of the control sample on the same blot. In this way, differences between blots in terms of blotting efficiency, antibody binding, and detection were taken into account.

Sporulation time-course experiments—Sporulation was induced in flasks and at 2 h PS culture aliquots (200 μL) were transferred to a 96-well plate (black walls, clear bottom). For experiments in which luminescence intensity was measured, for each biological replicate, three aliquots were added to wells containing D-luciferin (4.5 mM final concentration). Luminescence intensity was measured at intervals and averaged for the three wells. For experiments in which the Luc H245F level was also measured, for each biological replicate, seven aliquots were added to wells lacking luciferin (as a cost-saving measure since luciferin is expensive) and at intervals, a sample was collected for subsequent immunoblot analysis with anti-Luc antibodies as described above. A control experiment showed that luciferin did not affect the Luc H245F level. At each interval, the average luminescence intensity was divided by the Luc H245F level to yield a normalized value representing the relative ATP concentration for that biological replicate. Some samples subjected to immunoblot analysis with anti-Luc antibodies were also subjected to immunoblot analysis with other antibodies (Fig. 5 and 7A) as described above.

For the sporulation time-course experiment shown in Figure 8A, samples for immunoblot analysis were collected from flasks as described above, rather than from 96-well plates.

Fluorescence microscopy—The lipophilic dye FM 4-64 (AAT Bioquest) was used to stain membranes. Sporulation was induced in flasks and at 2 h PS culture aliquots were transferred to a 96-well plate with FM 4-64 (1 μg/mL final concentration), which does not affect sporulation. At intervals, an aliquot was collected and frozen in liquid nitrogen or examined immediately using a conventional fluorescence microscope. In several experiments, freezing of samples had no effect and the *spoIIQ* and *spoIIIAH* mutants were impaired for engulfment, whereas the WT strains and the *spoIIIAA* mutants (i.e. the two strains in each case, expressing *luc H245F* in the MC or FS) reproducibly progressed to the late stage and completion of engulfment with normal timing, based on qualitative observations.

For the representative experiments shown in Figure 4 and Table 1, sporulation was induced in flasks, at 2 h PS culture aliquots were transferred to a 96-well plate with FM 4-64, and at intervals, aliquots were frozen as described above. Imaging was performed on an Olympus FluoView FV-1000 filter-based confocal microscope. FM 4-64 (ex/em ~515/640 nm) was excited using a 515 nM argon laser and fluorescence was captured using a BA560IF band pass filter. A differential interference contrast image was also captured in order to score cells based on the presence of a phase-bright forespore, indicative of completed engulfment. For each sample, 150-250 cells were classified according to their morphological stage. For the channel mutants, only a sample at 6 h PS was examined (Table 1).

For the experiment shown in Figure 8B, sporulation was induced in flasks and at 3 h PS samples were collected, FM 4-64 was added to stain membranes, samples were frozen in liquid nitrogen, and imaging of fluorescence was performed as described above.

Supplementary Material

Refer to Web version on PubMed Central for supplementary material.

Acknowledgments

We thank Emily Frankman for constructing pEF1 and pEF2. We are grateful to David Rudner for providing antibodies against SpoIIQ and SpoIIIAH, and several strains of *B. subtilis* and plasmids. We also thank Kit Pogliano, Stephen Leppla, Hiromi Imamura, and Alan Grossman for sending strains and/or plasmids. We thank Amy Camp for helpful discussions, Kristin Parent for use of her plate reader, and Bob Hausinger for helpful comments on the manuscript. Fluorescence microscopy was performed at the Michigan State University Center for Advanced Microscopy. This research was supported by National Institutes of Health Grant R01 GM43585 and by Michigan State University AgBioResearch.

References

Arrieta-Ortiz ML, Hafemeister C, Bate AR, Chu T, Greenfield A, Shuster B, Barry SN, Gallitto M, Liu B, Kacmarczyk T, Santoriello F, Chen J, Rodrigues CD, Sato T, Rudner DZ, Driks A, Bonneau R, and Eichenberger P (2015) An experimentally supported model of the Bacillus subtilis global transcriptional regulatory network. Mol. Syst. Biol 11: 839. [PubMed: 26577401]

Baykov AA, Tuominen HK, and Lahti R (2011) The CBS domain: a protein module with an emerging prominent role in regulation. ACS Chem. Biol 6: 1156–1163. [PubMed: 21958115]

Blaylock B, Jiang X, Rubio A, Moran CP Jr., and Pogliano K (2004) Zipper-like interaction between proteins in adjacent daughter cells mediates protein localization. Genes Dev. 18: 2916–2928. [PubMed: 15574594]

Bradshaw N, and Losick R (2015) Asymmetric division triggers cell-specific gene expression through coupled capture and stabilization of a phosphatase. eLife 4: e08145. [PubMed: 26465112]

Branchini BR, Magyar RA, Murtiashaw MH, Anderson SM, Helgerson LC, and Zimmer M (1999) Site-directed mutagenesis of firefly luciferase active site amino acids: a proposed model for bioluminescence color. Biochemistry 38: 13223–13230. [PubMed: 10529195]

Broder DH, and Pogliano K (2006) Forespore engulfment mediated by a ratchet-like mechanism. Cell 126: 917–928. [PubMed: 16959571]

Bron S, (1990) Plasmids In: Molecular Biological Methods for Bacillus. Harwood CR & Cutting SM (eds). New York: John Wiley & Sons, pp. 75–174.

Camp AH, and Losick R (2008) A novel pathway of intercellular signalling in Bacillus subtilis involves a protein with similarity to a component of type III secretion channels. Mol. Microbiol 69: 402–417. [PubMed: 18485064]

Camp AH, and Losick R (2009) A feeding tube model for activation of a cell-specific transcription factor during sporulation in Bacillus subtilis. Genes Dev. 23: 1014–1024. [PubMed: 19390092]

Campo N, Marquis KA, and Rudner DZ (2008) SpoIIQ anchors membrane proteins on both sides of the sporulation septum in Bacillus subtilis. J. Biol. Chem 283: 4975–4982. [PubMed: 18077456]

Campo N, and Rudner DZ (2006) A branched pathway governing the activation of a developmental transcription factor by regulated intramembrane proteolysis. Mol. Cell 23: 25–35. [PubMed: 16818230]

Campo N, and Rudner DZ (2007) SpoIVB and CtpB are both forespore signals in the activation of the sporulation transcription factor σK in Bacillus subtilis. J. Bacteriol 189: 6021–6027. [PubMed: 17557826]

Chiba S, Coleman K, and Pogliano K (2007) Impact of membrane fusion and proteolysis on SpoIIQ dynamics and interaction with SpoIIIAH. J. Biol. Chem 282: 2576–2586. [PubMed: 17121846]

Clarke S, Lopez-Diaz I, and Mandelstam J (1986) Use of lacZ fusions to determine the dependence pattern of the sporulation gene spoIID in spo mutants of Bacillus subtilis. J. Gen. Microbiol 132: 2987–2994. [PubMed: 3114421]

Cutting S, Driks A, Schmidt R, Kunkel B, and Losick R (1991a) Forespore-specific transcription of a gene in the signal transduction pathway that governs pro-σK processing in Bacillus subtilis. Genes Dev. 5: 456–466. [PubMed: 1900494]

Cutting S, Oke V, Driks A, Losick R, Lu S, and Kroos L (1990) A forespore checkpoint for mother-cell gene expression during development in Bacillus subtilis. Cell 62: 239–250. [PubMed: 2115401]

Cutting S, Roels S, and Losick R (1991b) Sporulation operon spoIVF and the characterization of mutations that uncouple mother-cell from forespore gene expression in Bacillus subtilis. J. Mol. Biol 221: 1237–1256. [PubMed: 1942049]

Di Tomaso G, Borghese R, and Zannoni D (2001) Assay of ATP in intact cells of the facultative phototroph Rhodobacter capsulatus expressing recombinant firefly luciferase. Arch. Microbiol 177: 11–19. [PubMed: 11797039]

Doan T, Marquis KA, and Rudner DZ (2005) Subcellular localization of a sporulation membrane protein is achieved through a network of interactions along and across the septum. Mol. Microbiol 55: 1767–1781. [PubMed: 15752199]

Doan T, Morlot C, Meisner J, Serrano M, Henriques AO, Moran CP Jr., and Rudner DZ (2009) Novel secretion apparatus maintains spore integrity and developmental gene expression in Bacillus subtilis. PLoS Genet. 5: e1000566. [PubMed: 19609349]

Doan T, and Rudner DZ (2007) Perturbations to engulfment trigger a degradative response that prevents cell-cell signalling during sporulation in Bacillus subtilis. Mol. Microbiol 64: 500–511. [PubMed: 17493131]

Eichenberger P, Fujita M, Jensen ST, Conlon EM, Rudner DZ, Wang ST, Ferguson C, Haga K, Sato T, Liu JS, and Losick R (2004) The program of gene transcription for a single differentiating cell type during sporulation in Bacillus subtilis. PLoS Biol. 2: e328. [PubMed: 15383836]

Fimlaid KA, Jensen O, Donnelly ML, Siegrist MS, and Shen A (2015) Regulation of Clostridium difficile Spore Formation by the SpoIIQ and SpoIIIA Proteins. PLoS Genet. 11: e1005562. [PubMed: 26465937]

Flanagan KA, Comber JD, Mearls E, Fenton C, Wang Erickson AF, and Camp AH (2016) A membrane-embedded amino acid couples the SpoIIQ channel protein to anti-sigma factor transcriptional repression during Bacillus subtilis sporulation. J. Bacteriol 198: 1451–1463. [PubMed: 26929302]

Green D, and Cutting S (2000) Membrane topology of the Bacillus subtilis Pro-σK processing complex. J. Bacteriol 182: 278–285. [PubMed: 10629171]

Halder S, Parrell D, Whitten D, Feig M, and Kroos L (2017) Interaction of intramembrane metalloprotease SpoIVFB with substrate Pro-σK. Proc. Natl. Acad. Sci. USA 114: E10677–E10686. [PubMed: 29180425]

Harwood CR, and Cutting SM, (1990) Molecular Biological Methods for Bacillus, p. 581 John Wiley & Sons, Chichester, England.

Higgins D, and Dworkin J (2012) Recent progress in Bacillus subtilis sporulation. FEMS Microbiol. Rev 36: 131–148. [PubMed: 22091839]

Imamura H, Nhat KP, Togawa H, Saito K, Iino R, Kato-Yamada Y, Nagai T, and Noji H (2009) Visualization of ATP levels inside single living cells with fluorescence resonance energy transfer-based genetically encoded indicators. Proc. Natl. Acad. Sci. USA 106: 15651–15656. [PubMed: 19720993]

Jiang X, Rubio A, Chiba S, and Pogliano K (2005) Engulfment-regulated proteolysis of SpoIIQ: evidence that dual checkpoints control sigma activity. Mol. Microbiol 58: 102–115. [PubMed: 16164552]

Jordan S, Hutchings MI, and Mascher T (2008) Cell envelope stress response in Gram-positive bacteria. FEMS Microbiol. Rev 32: 107–146. [PubMed: 18173394]

Karmazyn-Campelli C, Bonamy C, Savelli B, and Stragier P (1989) Tandem genes encoding σ-factors for consecutive steps of development in Bacillus subtilis. Genes & Dev. 3: 150–157. [PubMed: 2497052]

Konovalova A, Sogaard-Andersen L, and Kroos L (2014) Regulated proteolysis in bacterial development. FEMS Microbiol. Rev 38: 493–522. [PubMed: 24354618]

Kroos L (2007) The Bacillus and Myxococcus developmental networks and their transcriptional regulators. Annu. Rev. Genet 41: 13–39. [PubMed: 18076324]

Kroos L, and Akiyama Y (2013) Biochemical and structural insights into intramembrane metalloprotease mechanisms. Biochim. Biophys. Acta - Biomembr 1828: 2873–2885.

Kroos L, Yu YT, Mills D, and Ferguson-Miller S (2002) Forespore signaling is necessary for pro-σK processing during Bacillus subtilis sporulation despite the loss of SpoIVFA upon translational arrest. J. Bacteriol 184: 5393–5401. [PubMed: 12218026]

Levdikov VM, Blagova EV, McFeat A, Fogg MJ, Wilson KS, and Wilkinson AJ (2012) Structure of components of an intercellular channel complex in sporulating Bacillus subtilis. Proc. Natl. Acad. Sci. USA 109: 5441–5445. [PubMed: 22431604]

Londono-Vallejo JA (1997) Mutational analysis of the early forespore/mother-cell signalling pathway in Bacillus subtilis. Microbiol. 143: 2753–2761.

Londono-Vallejo JA, Frehel C, and Stragier P (1997) SpoIIQ, a forespore-expressed gene required for engulfment in Bacillus subtilis. Mol. Microbiol 24: 29–39. [PubMed: 9140963]

Losick R, and Stragier P (1992) Crisscross regulation of cell-type-specific gene expression during development in B. subtilis. Nature 355: 601–604. [PubMed: 1538747]

Lu S, Halberg R, and Kroos L (1990) Processing of the mother-cell σ factor, σK, may depend on events occurring in the forespore during Bacillus subtilis development. Proc. Natl. Acad. Sci. USA 87: 9722–9726. [PubMed: 2124700]

McElroy WD (1947) The energy source for bioluminescence in an isolated system. Proc. Natl. Acad. Sci. USA 33: 342–345. [PubMed: 16588763]

Mearls EB, Jackter J, Colquhoun JM, Farmer V, Matthews AJ, Murphy LS, Fenton C, and Camp AH (2018) Transcription and translation of the sigG gene is tuned for proper execution of the switch from early to late gene expression in the developing Bacillus subtilis spore. PLoS Genet. 14: e1007350. [PubMed: 29702640]

Meisner J, Maehigashi T, Andre I, Dunham CM, and Moran CP Jr. (2012) Structure of the basal components of a bacterial transporter. Proc. Natl. Acad. Sci. USA 109: 5446–5451. [PubMed: 22431613]

Meisner J, Wang X, Serrano M, Henriques AO, and Moran CP Jr. (2008) A channel connecting the mother cell and forespore during bacterial endospore formation. Proc. Natl. Acad. Sci. USA 105: 15100–15105. [PubMed: 18812514]

Mirouze N, Prepiak P, and Dubnau D (2011) Fluctuations in spo0A transcription control rare developmental transitions in Bacillus subtilis. PLoS Genet. 7: e1002048. [PubMed: 21552330]

Ramirez-Guadiana FH, Rodrigues CDA, Marquis KA, Campo N, Barajas-Ornelas RDC, Brock K, Marks DS, Kruse AC, and Rudner DZ (2018) Evidence that regulation of intramembrane proteolysis is mediated by substrate gating during sporulation in Bacillus subtilis. PLoS Genet. 14: e1007753. [PubMed: 30403663]

Ricca E, Cutting S, and Losick R (1992) Characterization of bofA, a gene involved in intercompartmental regulation of pro-σK processing during sporulation in Bacillus subtilis. J. Bacteriol 174: 3177–3184. [PubMed: 1577688]

Rodrigues CD, Henry X, Neumann E, Kurauskas V, Bellard L, Fichou Y, Schanda P, Schoehn G, Rudner DZ, and Morlot C (2016a) A ring-shaped conduit connects the mother cell and forespore during sporulation in Bacillus subtilis. Proc. Natl. Acad. Sci. USA 113: 11585–11590. [PubMed: 27681621]

Rodrigues CD, Ramirez-Guadiana FH, Meeske AJ, Wang X, and Rudner DZ (2016b) GerM is required to assemble the basal platform of the SpoIIIA-SpoIIQ transenvelope complex during sporulation in Bacillus subtilis. Mol. Microbiol 102: 260–273. [PubMed: 27381174]

Rudner D, Fawcett P, and Losick R (1999) A family of membrane-embedded metalloproteases involved in regulated proteolysis of membrane-associated transcription factors. Proc. Natl. Acad. Sci. USA 96: 14765–14770. [PubMed: 10611287]

Rudner DZ, and Losick R (2002) A sporulation membrane protein tethers the pro-σK processing enzyme to its inhibitor and dictates its subcellular localization. Genes Dev. 16: 1007–1018. [PubMed: 11959848]

Schneider DA, and Gourse RL (2004) Relationship between growth rate and ATP concentration in Escherichia coli: a bioassay for available cellular ATP. J. Biol. Chem 279: 8262–8268. [PubMed: 14670952]

Scott JW, Hawley SA, Green KA, Anis M, Stewart G, Scullion GA, Norman DG, and Hardie DG (2004) CBS domains form energy-sensing modules whose binding of adenosine ligands is disrupted by disease mutations. J. Clin. Invest 113: 274–284. [PubMed: 14722619]

Serrano M, Crawshaw AD, Dembek M, Monteiro JM, Pereira FC, Pinho MG, Fairweather NF, Salgado PS, and Henriques AO (2016) The SpoIIQ-SpoIIIAH complex of Clostridium difficile controls forespore engulfment and late stages of gene expression and spore morphogenesis. Mol. Microbiol 100: 204–228. [PubMed: 26690930]

Serrano M, Gao J, Bota J, Bate AR, Meisner J, Eichenberger P, Moran CP Jr., and Henriques AO (2015) Dual-specificity anti-sigma factor reinforces control of cell-type specific gene expression in Bacillus subtilis. PLoS Genet. 11: e1005104. [PubMed: 25835496]

Setlow P, and Kornberg A (1970) Biochemical studies of bacterial sporulation and germination. XXII. Energy metabolism in early stages of germination of Bacillus megaterium spores. J. Biol. Chem 245: 3637–3644. [PubMed: 4394282]

Setlow P, and Primus G (1975) Protein metabolism during germination of Bacillus megaterium spores. I. Protein synthesis and amino acid metabolism. J. Biol. Chem 250: 623–630. [PubMed: 803494]

Sharp MD, and Pogliano K (2002) Role of cell-specific SpoIIIE assembly in polarity of DNA transfer. Science 295: 137–139. [PubMed: 11778051]

Shimotsu H, and Henner DJ (1986) Construction of a single-copy integration vector and its use in analysis of regulation of the trp operon of Bacillus subtilis. Gene 43: 85–94. [PubMed: 3019840]

Singh RP, Setlow B, and Setlow P (1977) Levels of small molecules and enzymes in the mother cell compartment and the forespore of sporulating Bacillus megaterium. J. Bacteriol 130: 1130–1138. [PubMed: 193830]

Sterlini JM, and Mandelstam J (1969) Commitment to sporulation in Bacillus subtilis and its relationship to development of actinomycin resistance. Biochem. J 113: 29–37. [PubMed: 4185146]

Strahl H, and Hamoen LW (2010) Membrane potential is important for bacterial cell division. Proc. Natl. Acad. Sci. USA 107: 12281–12286. [PubMed: 20566861]

Sun YL, Sharp MD, and Pogliano K (2000) A dispensable role for forespore-specific gene expression in engulfment of the forespore during sporulation of Bacillus subtilis. J. Bacteriol 182: 2919–2927. [PubMed: 10781563]

Tan IS, and Ramamurthi KS (2014) Spore formation in Bacillus subtilis. Environ. Microbiol. Rep 6: 212–225. [PubMed: 24983526]

Trouve J, Mohamed A, Leisico F, Contreras-Martel C, Liu B, Mas C, Rudner DZ, Rodrigues CDA, and Morlot C (2018) Structural characterization of the sporulation protein GerM from Bacillus subtilis. J. Struct. Biol 204: 481–490. [PubMed: 30266596]

Wakeley PR, Dorazi R, Hoa NT, Bowyer JR, and Cutting SM (2000) Proteolysis of SpoIVB is a critical determinant in signalling of Pro-σK processing in Bacillus subtilis. Mol. Microbiol 36: 1336–1348. [PubMed: 10931284]

Wang L, Perpich J, Driks A, and Kroos L (2007) One perturbation of the mother cell gene regulatory network suppresses the effects of another during sporulation of Bacillus subtilis. J. Bacteriol 189: 8467–8473. [PubMed: 17890309]

Yu Y-TN, and Kroos L (2000) Evidence that SpoIVFB is a novel type of membrane metalloprotease governing intercompartmental communication during Bacillus subtilis sporulation. J. Bacteriol 182: 3305–3309. [PubMed: 10809718]

Zeytuni N, Flanagan KA, Worrall LJ, Massoni SC, Camp AH, and Strynadka NCJ (2018) Structural characterization of SpoIIIAB sporulation-essential protein in Bacillus subtilis. J Struct Biol 202: 105–112. [PubMed: 29288127]

Zeytuni N, Hong C, Flanagan KA, Worrall LJ, Theiltges KA, Vuckovic M, Huang RK, Massoni SC, Camp AH, Yu Z, and Strynadka NC (2017) Near-atomic resolution cryoelectron microscopy structure of the 30-fold homooligomeric SpoIIIAG channel essential to spore formation in Bacillus subtilis. Proc. Natl. Acad. Sci. USA 114: E7073–E7081. [PubMed: 28784753]

Zhang B, and Kroos L (1997) A feedback loop regulates the switch from one sigma factor to the next in the cascade controlling Bacillus subtilis mother cell gene expression. J. Bacteriol 179: 6138–6144. [PubMed: 9324264]

Zhang B, Struffi P, and Kroos L (1999) σK can negatively regulate sigE expression by two different mechanisms during sporulation of Bacillus subtilis. J. Bacteriol 181: 4081–4088. [PubMed: 10383978]

Zhang Y, Halder S, Kerr R, Parrell D, Ruotolo B, and Kroos L (2016) Complex formed between intramembrane metalloprotease SpoIVFB and its substrate, Pro-σK. J. Biol. Chem 291: 10347–10362. [PubMed: 26953342]

Zhang Y, Luethy PM, Zhou R, and Kroos L (2013) Residues in conserved loops of intramembrane metalloprotease SpoIVFB interact with residues near the cleavage site in Pro-σK. J. Bacteriol 195: 4936–4946. [PubMed: 23995631]

Zhou R, Cusumano C, Sui D, Garavito RM, and Kroos L (2009) Intramembrane proteolytic cleavage of a membrane-tethered transcription factor by a metalloprotease depends on ATP. Proc. Natl. Acad. Sci. USA 106: 16174–16179. [PubMed: 19805276]

Zhou R, and Kroos L (2004) BofA protein inhibits intramembrane proteolysis of pro-σK in an intercompartmental signaling pathway during Bacillus subtilis sporulation. Proc. Natl. Acad. Sci. USA 101: 6385–6390. [PubMed: 15087499]

Zhou R, and Kroos L (2005) Serine proteases from two cell types target different components of a complex that governs regulated intramembrane proteolysis of pro-σK during Bacillus subtilis development. Mol. Microbiol 58: 835–846. [PubMed: 16238631]

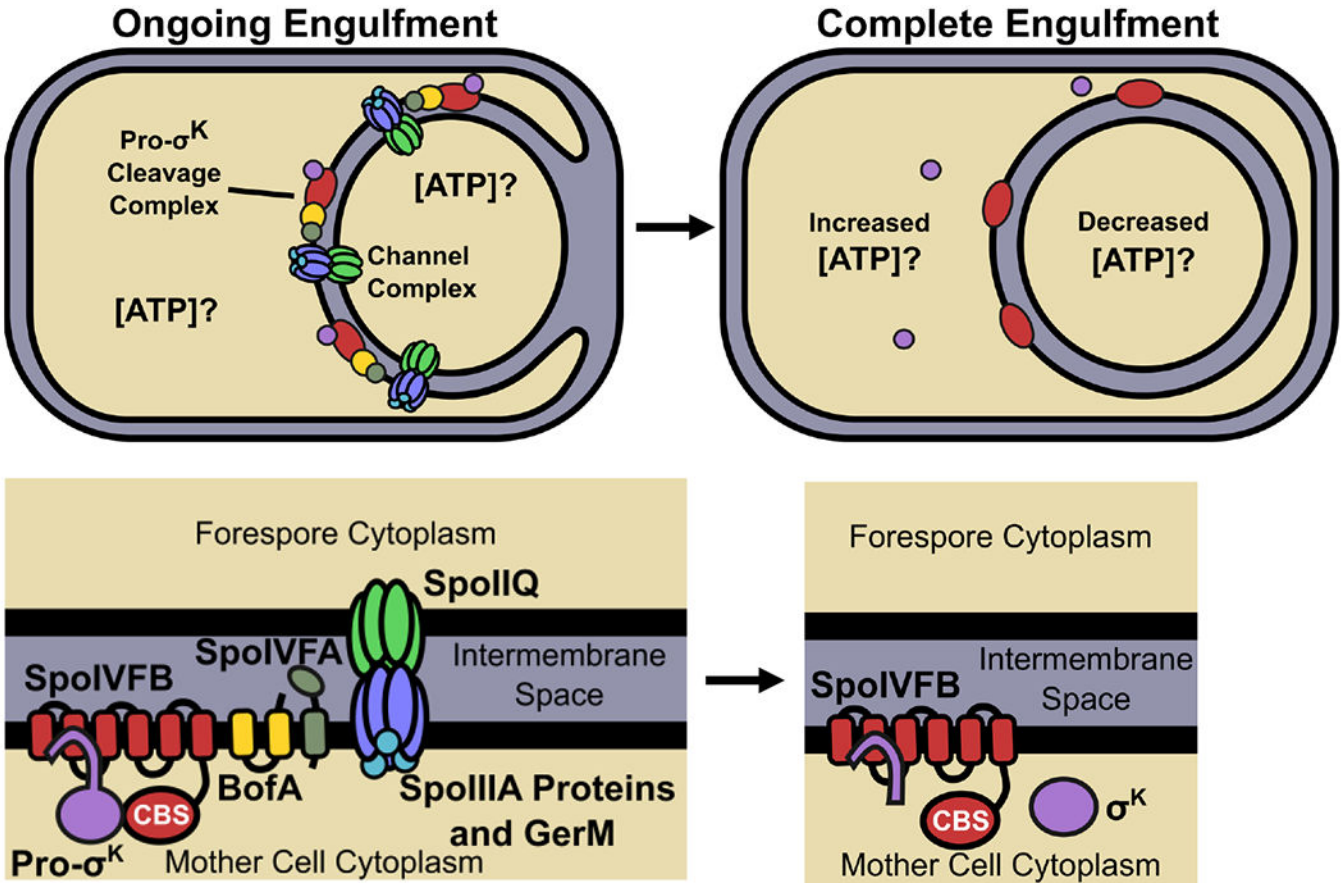

Fig. 1. Model for how channels may impact ATP concentrations and Pro-σ^K cleavage.

The top left panel illustrates ongoing engulfment, during which the MC membrane migrates around the FS and active channel complexes form (Blaylock et al., 2004, Camp & Losick, 2008, Meisner et al., 2008, Camp & Losick, 2009, Doan et al., 2009). A possible function of the channels is to maintain a similar ATP concentration in the two compartments. Inactive Pro-σ^K cleavage complexes are associated with channel complexes (Doan et al., 2005, Jiang et al., 2005). The bottom left panel indicates the proteins in each complex. The top right panel illustrates complete engulfment. The FS has been pinched off within the MC. Channel complexes are inactive or absent (the latter is depicted) (Meisner et al., 2008, Doan et al., 2009, Chiba et al., 2007). The lack of channel function may cause the MC ATP concentration to increase. Gene expression in the FS may cause the ATP concentration to decrease. SpoIVB and CtpB produced under σ^G control in the FS (not shown) are secreted into the intermembrane space and cleave SpoIVFA and BofA (depicted as absent), relieving inhibition of SpoIVFB (Cutting et al., 1991a, Wakeley et al., 2000, Zhou & Kroos, 2005, Campo & Rudner, 2006, Campo & Rudner, 2007, Cutting et al., 1990, Cutting et al., 1991b, Ricca et al., 1992, Rudner & Losick, 2002, Zhou & Kroos, 2004). The CBS domain of SpoIVFB (bottom right) may sense the elevated ATP concentration in the MC (Zhou et al., 2009), so that Pro-σ^K is cleaved and σ^K is released into the MC.

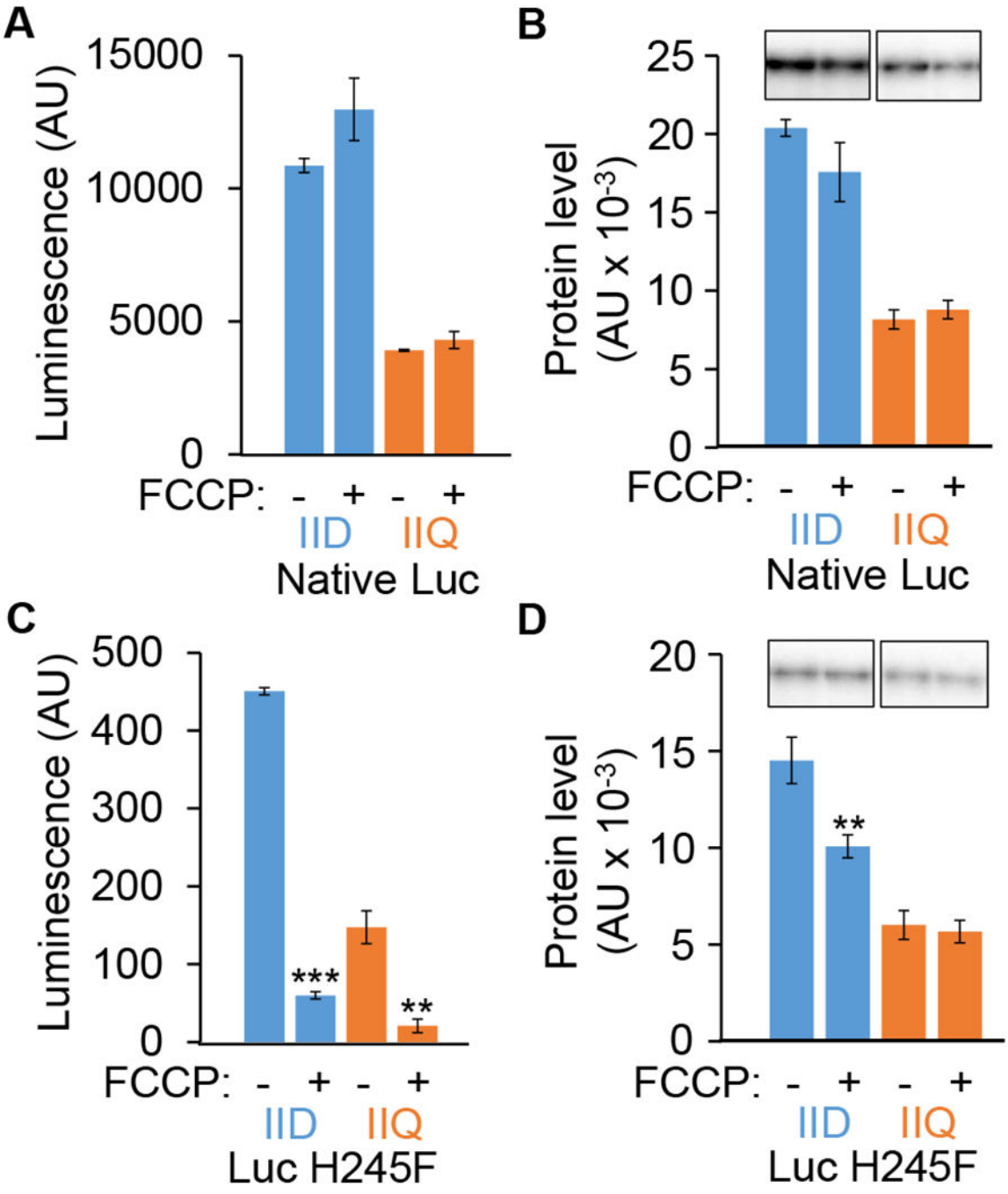

Fig. 2. Luc H245F detects decreases in compartment-specific luminescence intensity after FCCP treatment during sporulation.

B. subtilis strains engineered to express the genes encoding native Luc or Luc H245F in the MC or FS were starved to induce sporulation. At 3.5 h PS, culture aliquots were transferred to a 96-well plate containing luciferin. Aliquots were left untreated as controls (−) or were treated with 100 μM FCCP (+) for 15 min, prior to measuring the luminescence intensity in arbitrary units (AU) and the Luc level in AU by immunoblot analysis with anti-Luc antibodies. Each Luc signal was quantified and normalized to a control sample on the same blot. Graphs show the average of three biological replicates and error bars represent one

standard deviation. Two asterisks (**) indicate $P < 0.005$ and three asterisks (***) indicate $P < 0.0005$ in paired two-tailed *t*-tests comparing the data for the untreated control with the FCCP-treated sample. Luminescence intensity from native Luc **(A)** and Luc H245F **(C)**. Levels of native Luc **(B)** and Luc H245F **(D)**. Representative immunoblots are shown at the top and quantification of replicates is shown below.

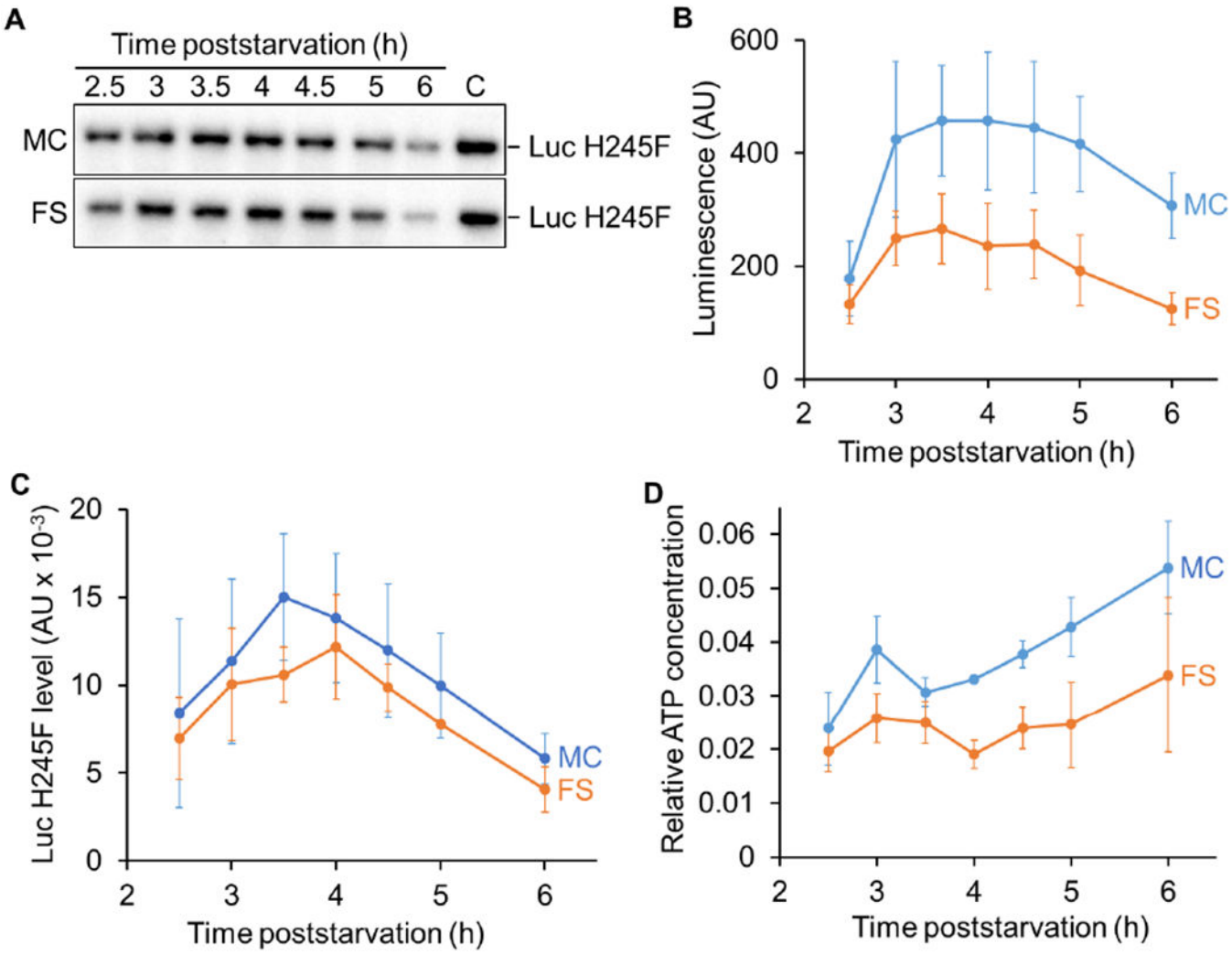

Fig. 3. The relative ATP concentration rises in the mother cell and does not decline in the forespore during sporulation.

B. subtilis strains engineered to express *luc H245F* in the MC or the FS were starved to induce sporulation. At 2 h PS, culture aliquots were transferred to a 96-well plate, prior to measuring the luminescence intensity in arbitrary units (AU) and the Luc H245F level in AU by immunoblot analysis with anti-Luc antibodies. **(A)** Representative immunoblots showing Luc H245F levels in the MC and the FS during sporulation. A control sample (C) on the same blot was used for normalization of signal intensities. **(B)** Luminescence from Luc H245F synthesized in the MC or the FS during sporulation. **(C)** Luc H245F levels in the MC and the FS during sporulation. Each Luc H245F signal was quantified and normalized to a control sample on the same blot. **(D)** Relative ATP concentration in the MC and the FS during sporulation. For each biological replicate, the luminescence intensity was divided by the Luc H245F level to yield a normalized value representing the relative ATP concentration. The graphs show the average of three biological replicates and error bars represent one standard deviation.

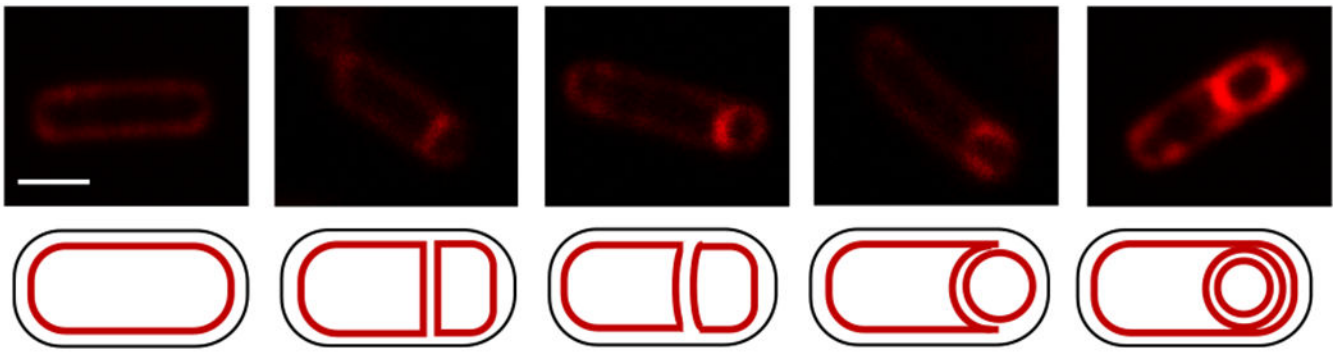

Time PS (h)	Percentage of sporangia at each morphological stage			
	Flat septa	Curved septa	Early engulfment	Late or complete engulfment
2.5	43	25	16	16
3	35	21	23	21
3.5	10	6	13	71
4	6	5	9	80
4.5	13	4	14	69
5	8	3	10	79
6	4	4	5	87

Fig. 4. Morphological changes during sporulation.

B. subtilis strains engineered to produce Luc H245F in the MC or FS were starved to induce sporulation. At 2 h PS, culture aliquots were transferred to a 96-well plate containing FM 4-64 to stain membranes. Images were collected at the indicated times PS using confocal fluorescence microscopy. A representative rod-shaped cell (top, left panel; scale bar = 1 μm) and sporangia representative of each stage (top row; same scale) are shown, with cartoon depictions of their membranes below. The percentage of sporangia (150-250 counted; rod-shaped cells were not counted) at each morphological stage is listed at each time PS for the strain producing Luc H245F in the MC. Gray fill indicates > 20%. Similar results were observed for the strain engineered to produce Luc H245F in the FS, and for the WT parental strain PY79 that does not produce Luc H245F.

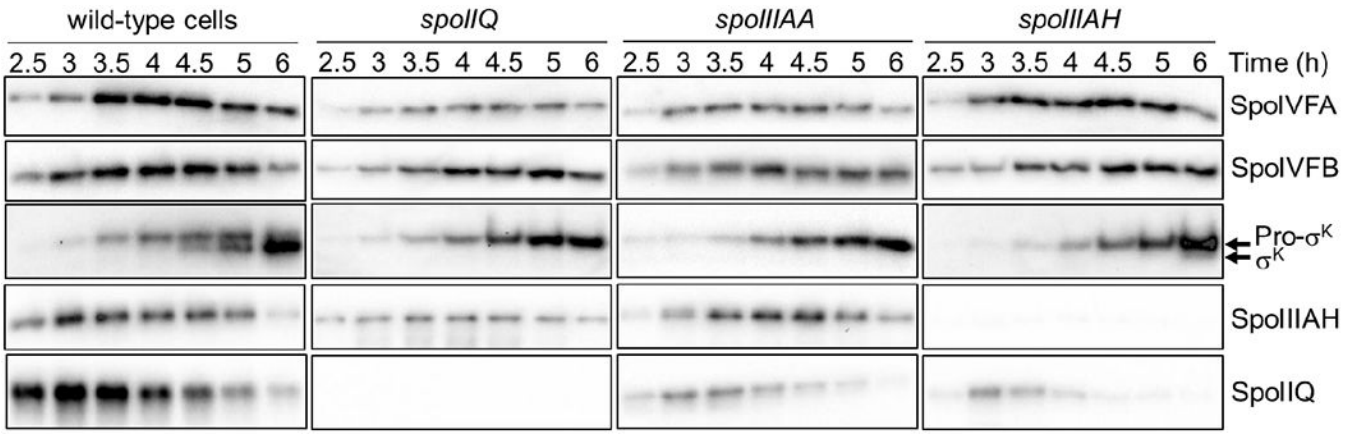

Fig. 5. Cleavage of Pro-σ^K and levels of channel proteins in wild-type cells and mutants deficient in channel proteins.

B. subtilis strains engineered to produce Luc H245F in the MC or FS were starved to induce sporulation. At 2 h PS, culture aliquots were transferred to a 96-well plate. Samples collected from aliquots at the indicated times PS were subjected to immunoblot analysis using antibodies against SpoIVFA, SpoIVFB, Pro-σ^K, SpoIIIAH, and SpoIIQ. Representative immunoblots are shown for WT cells and null mutants of the indicated channel proteins. Similar results were observed for at least two biological replicates of strains producing Luc H245F in the MC or FS.

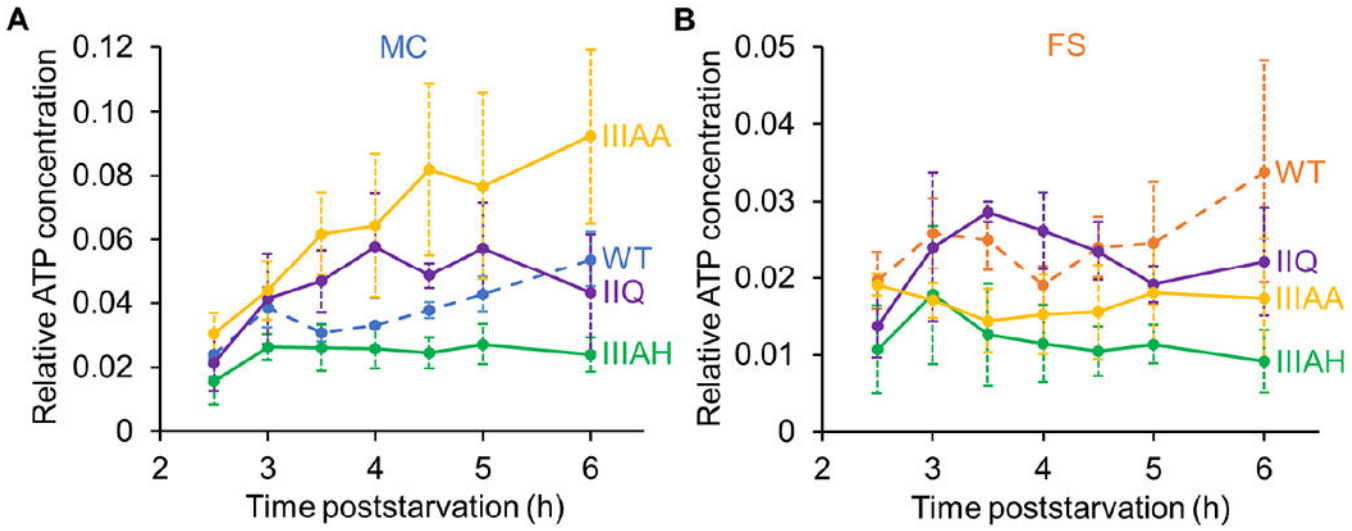

Fig. 6. Compartment-specific ATP concentration is altered in channel mutants.

B. subtilis mutants unable to produce the indicated channel protein and engineered to synthesize Luc H245F in the MC or FS were starved to induce sporulation. At 2 h PS, culture aliquots were transferred to a 96-well plate, and at the indicated times PS the luminescence intensity was measured (Fig. S7) and the Luc H245F level was assessed by immunoblot analysis with anti-Luc antibodies (Fig. S8). For each biological replicate, the luminescence intensity was divided by the Luc H245F level to yield a normalized value representing the relative ATP concentration in the MC **(A)** or FS **(B)**. Graphs show the average of three or four biological replicates and error bars represent one standard deviation. WT cell results are shown for comparison (same data as Fig. 3D). One asterisk (*) indicates $P < 0.05$ and two asterisks (**) indicate $P < 0.005$ in Student's two-tailed *t*-tests comparing the data for each mutant with WT cells at the same time PS.

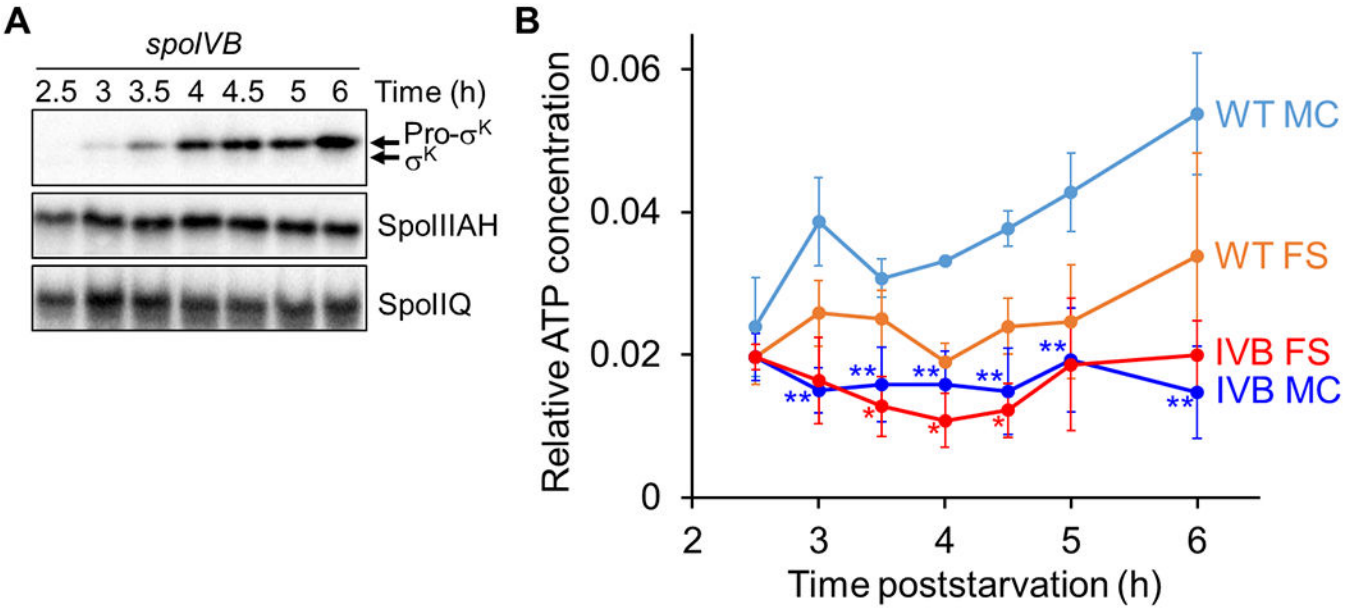

Fig. 7. Channel proteins persist in a *spoIVB* mutant and the ATP concentration remains low in both compartments.

B. subtilis strains unable to produce SpoIVB and engineered to produce Luc H245F in the MC or FS were starved to induce sporulation. At 2 h PS, culture aliquots were transferred to a 96-well plate, and at the indicated times PS the luminescence intensity was measured (Fig. S7) and the Luc H245F level was assessed by immunoblot analysis with anti-Luc antibodies (Fig. S8). Samples were also subjected to immunoblot analysis using antibodies against Pro-σ^K, SpoIIIAH, and SpoIIQ. **(A)** Protein levels during sporulation. Representative immunoblots are shown for the indicated proteins. Similar results were observed for at least two biological replicates of strains expressing Luc H245F in the MC or FS. **(B)** Relative ATP concentration in each compartment during sporulation. For each biological replicate, the luminescence intensity was divided by the Luc H245F level to yield a normalized value representing the relative ATP concentration in the MC or the FS as indicated. Graphs show the average of three biological replicates and error bars represent one standard deviation. WT cell results are shown for comparison (same data as Fig. 3D). One asterisk (*) indicates $P < 0.05$ and two asterisks (**) indicate $P < 0.005$ in Student's two-tailed *t*-tests comparing the data for each mutant with WT cells at the same time PS and in the same compartment.

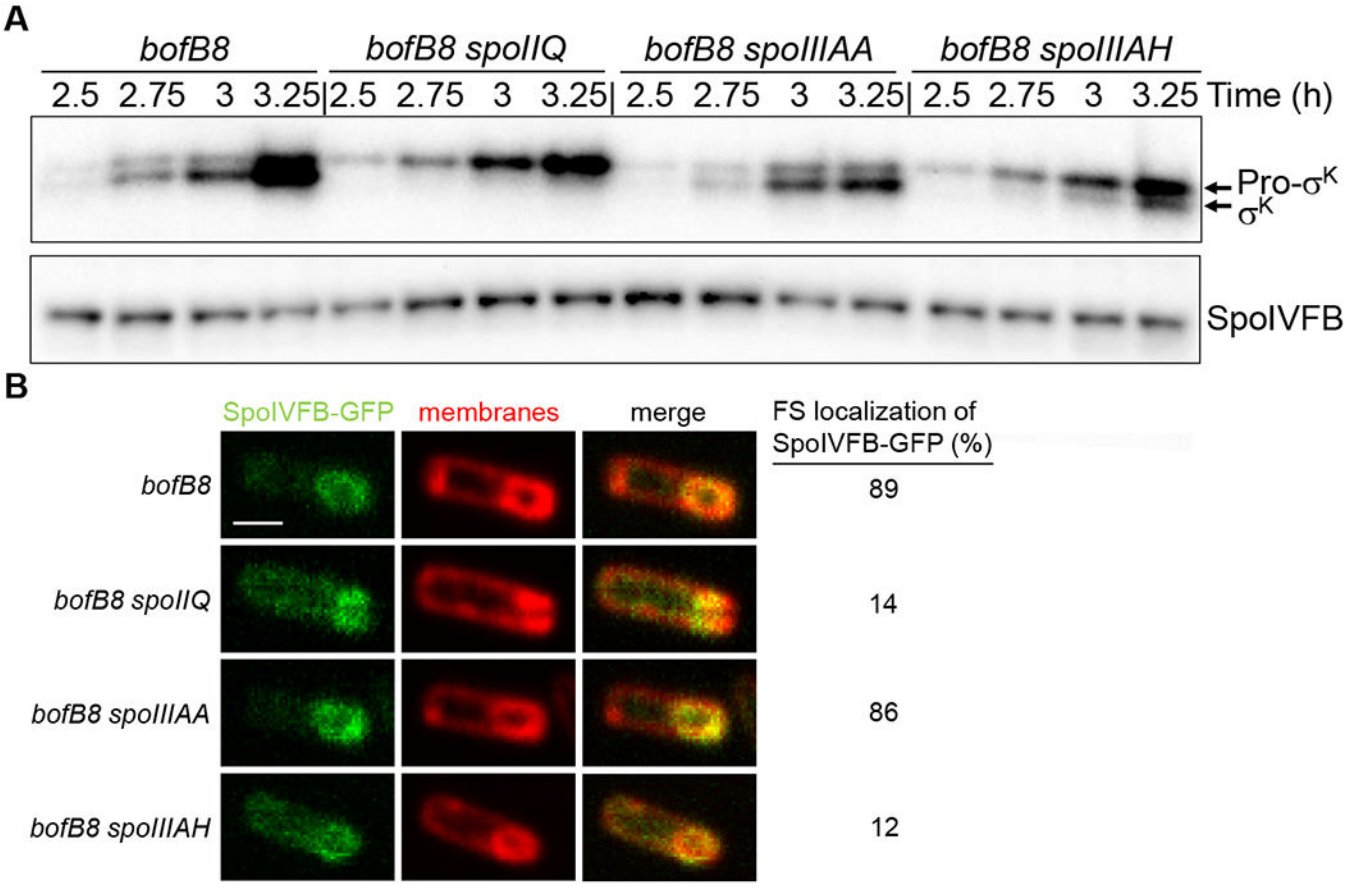

Fig. 8. Bypass mutants lacking channel proteins differ in cleavage of Pro-σ^K and SpoIVFB-GFP localization.

B. subtilis strains bearing the *bofB8* mutation alone or in combination with a null mutation in *spoIIQ*, *spoIIIAA*, or *spoIIIAH* were starved to induce sporulation. All these strains have a null mutation in *sigG*, which is bypassed by the *bofB8* mutation (Cutting et al., 1990). **(A)** Immunoblot analysis. Samples collected at the indicated times PS were subjected to immunoblot analysis using antibodies against Pro-σ^K and SpoIVFB. Representative immunoblots are shown. Similar results were observed for at least two biological replicates. **(B)** Confocal fluorescence microscopy. The native *spoIVFB* gene was C-terminally fused to *gfp* in the indicated strains, samples were collected at 3 h PS, and FM 4-64 was added to stain membranes. Images of fluorescence from SpoIVFB-GFP and membranes, and the merged images, are shown in the indicated columns, for representative sporangia with FS-localized (*bofB8* and *bofB8 spoIIIAA*) or mislocalized (*bofB8 spoIIQ* and *bofB8 spoIIIAH*) SpoIVFB-GFP. In the top, left panel the scale bar = 1 μm. The percentage of sporangia (100-150 counted; rod-shaped cells were not counted) with FS-localized SpoIVFB-GFP is shown in the rightmost column.

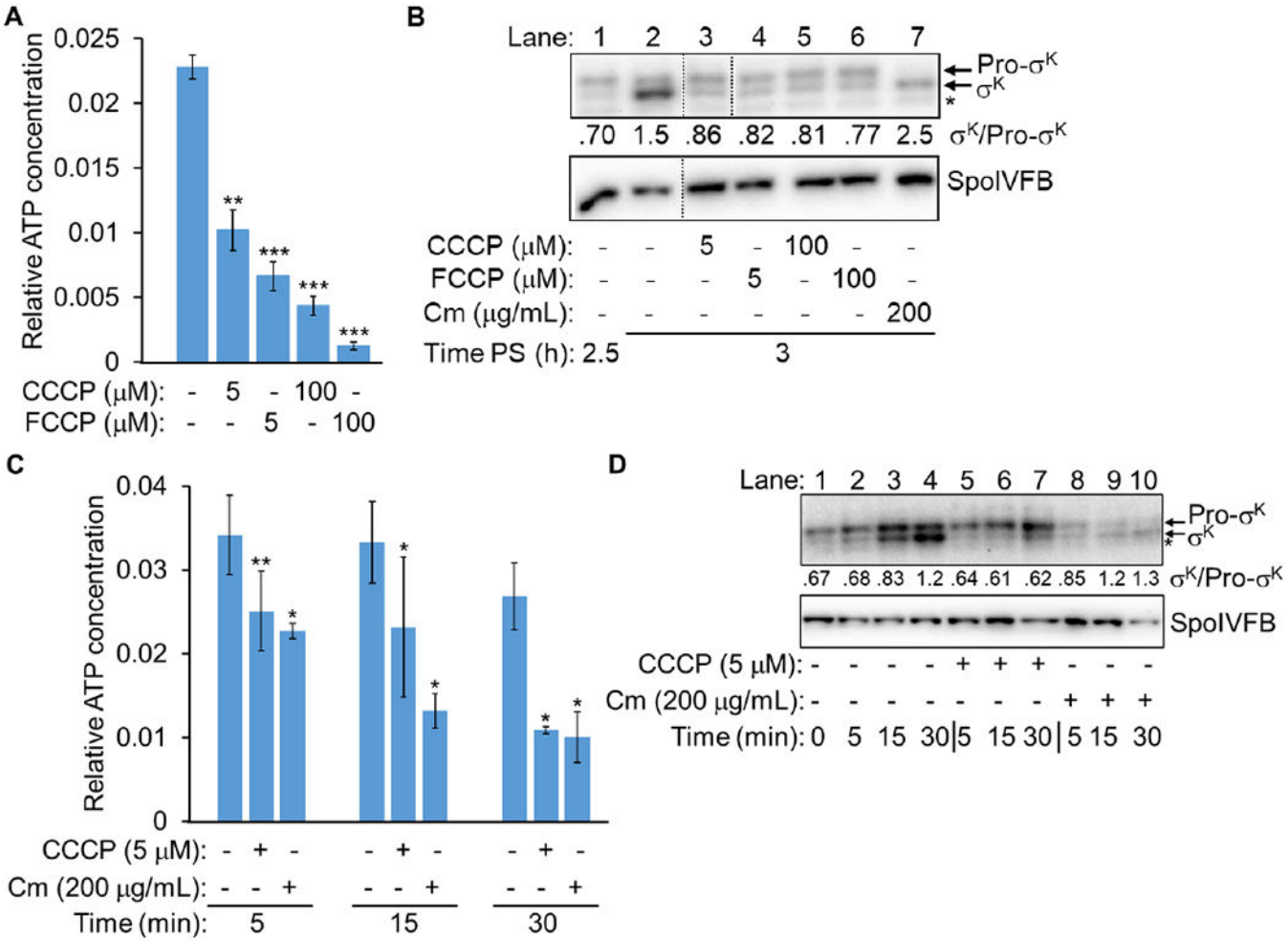

Fig. 9. Ionophores and chloramphenicol decrease the mother cell ATP concentration but allow Pro-σ^K cleavage.

(A) Relative ATP concentration in the MC after ionophore treatment. *B. subtilis* engineered to synthesize Luc H245F in the MC was starved to induce sporulation. At 3.5 h PS, culture aliquots were transferred to a 96-well plate containing luciferin. Aliquots were left untreated as controls (−) or were treated with an ionophore as indicated for 15 min, prior to measuring the luminescence intensity and the Luc H245F level by immunoblot analysis with anti-Luc antibodies (Fig. S11). For each biological replicate, the luminescence intensity was divided by the Luc H245F level to yield a normalized value representing the relative ATP concentration. The graph shows the average of three or four biological replicates and error bars represent one standard deviation. Two asterisks (**) indicate $P < 0.005$ and three asterisks (***) indicate $P < 0.0005$ in paired two-tailed *t*-tests comparing the data for the untreated control with the treated sample. **(B)** Cleavage of Pro-σ^K after ionophore or Cm treatment. *B. subtilis* with a null mutation in *sigG* and the *bofB8* mutation that bypasses the need for *sigG* (Cutting et al., 1990) was starved to induce sporulation. At 2.25 h PS, the culture was split, and at 2.5 h, the cultures were left untreated as a control (−) or were treated with an ionophore or Cm as indicated until 3 h. Samples were subjected to immunoblot analysis with antibodies against Pro-σ^K and SpoIVFB. A representative immunoblot is

shown (dotted lines indicate intervening lanes were removed from the blot). The asterisk indicates a breakdown product of Pro-σ^K or a cross-reactive protein. The σ^K and Pro-σ^K signal intensities were quantified (Table S1) and the ratio is shown. Similar results were observed for at least two biological replicates. **(C)** Relative ATP concentration in the MC after CCCP or Cm treatment. The experiment was performed as described for panel A, except at 2.5 h (to match panel B), aliquots were transferred to a 96-well plate containing luciferin. Aliquots were left untreated as controls (−) or were treated with CCCP or Cm as indicated for 5, 15, or 30 min, prior to measuring the luminescence intensity and the Luc H245F level (Fig. S13). For each biological replicate, the luminescence intensity was divided by the Luc H245F level to yield a normalized value representing the relative ATP concentration. The graph shows the average of three biological replicates and error bars represent one standard deviation. One asterisk (*) indicates $P \leq 0.05$ and two asterisks (**) indicate $P < 0.005$ in paired two-tailed *t*-tests comparing the data for the untreated control with the sample treated for the same amount of time. **(D)** Cleavage of Pro-σ^K after CCCP or Cm treatment. The experiment was performed as described for panel B, except cultures were left untreated as a control (−) or were treated as indicated for 5, 15, or 30 min.

Table 1

Morphology of bacterial strains after 6 h of starvation.

Strain[a]	Percentage of sporangia at each morphological stage			
	Flat septa	Curved septa	Early engulfment	Late or complete engulfment
WT	4	4	5	87
spoIIQ	13	7	59	21
spoIIIAH	9	12	42	37
spoIIIAA	8	5	4	83

[a] *B. subtilis* wild-type (WT) or mutant strains engineered to produce Luc H245F in the MC or FS were starved to induce sporulation. At 2 h PS, culture aliquots were transferred to a 96-well plate containing FM 4-64 to stain membranes. Images were collected at 6 h PS using confocal fluorescence microscopy. The percentage of sporangia (150-250 counted; rod-shaped cells were not counted) at each morphological stage is listed for the strains synthesizing Luc H245F in the MC. Data for WT cells are from Figure 4. Gray fill indicates > 40%. Similar results were observed for the strains synthesizing Luc H245F in the FS.